IEEE CSC & ESAS SUPERCONDUCTIVITY NEWS FORUM (global edition), February 2019.
Plenary presentation 3PL1A-01 given at ASC 2018, October 28-November 02, 2018, Seattle, (USA).

Microstructure -Property Correlations in Superconducting Wires

Peter J. Lee

With contributions from : David Larbalestier, Shreyas Balachandran, Chiara Tarantini, Anatolii Polyanskii, Fumitake Kametani, Bill Starch, and Yi-Feng Su

And past ASC graduate students: Jim McKinnell, Jeff Parrell, Christoph Meingast, Matt Jewell, Charlie Sanabria, Chris Segal and undergraduates Jonathon Cooper and Benjamin Walker

SEATTLE 2018
SEATTLE, 2018 OCTOBER 28 - NOVEMBER 2

ASC NATIONAL MAGLAB

Production Nb-Ti and Nb_3Sn J_cs have plateaued

- But significant increases in Nb_3Sn critical current density are required to reach FCC targets

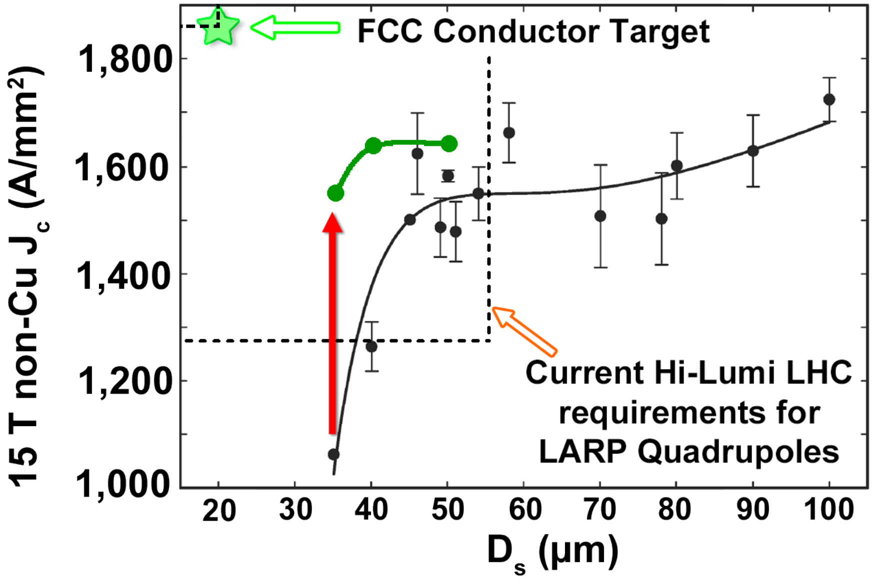

Charlie Sanabria et al 2018 Supercond. Sci. Technol. 31 064001

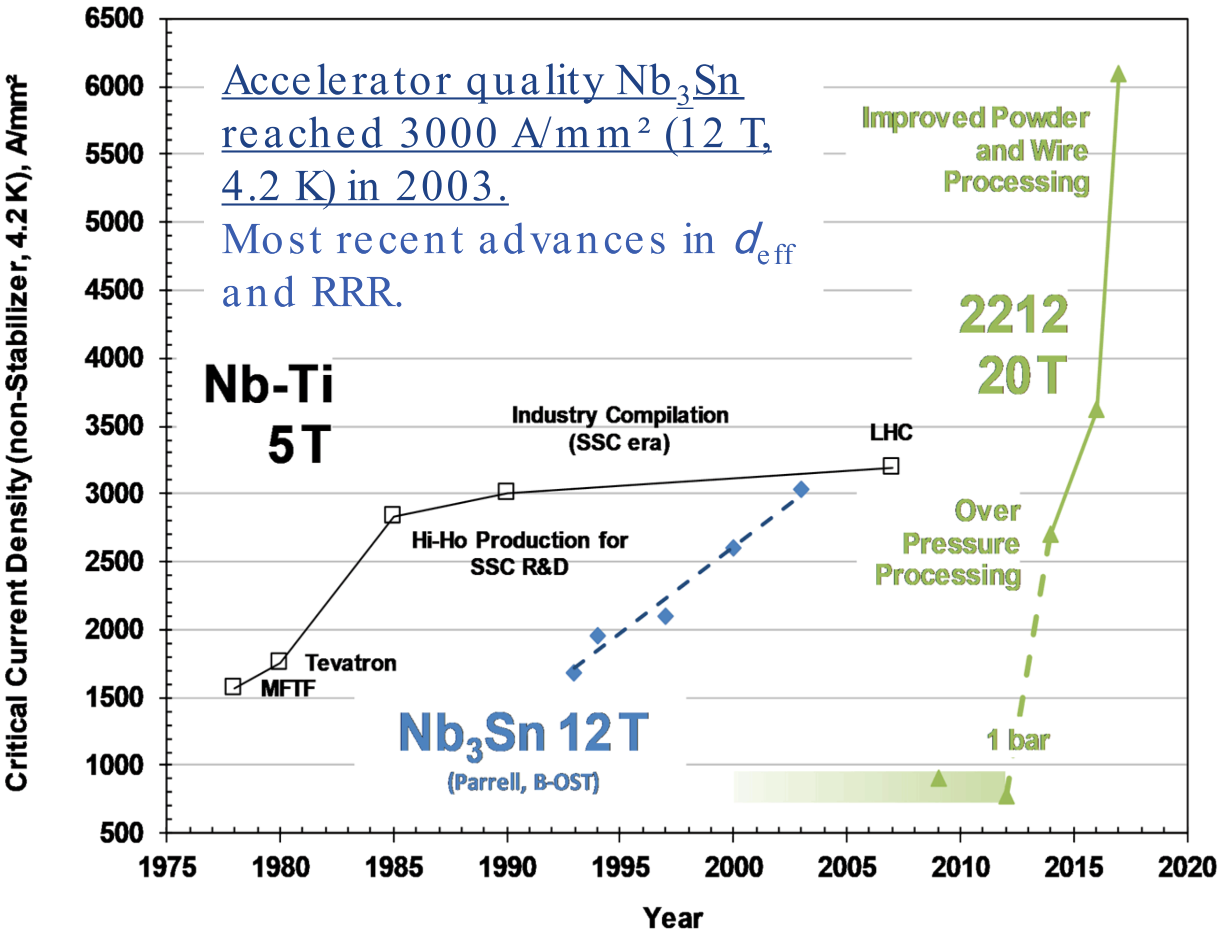

Nb_3Sn data: J. A. Parrell, Adv. Cryo. Eng. 50, pp. 369–375, 2004: http://dx.doi.org/10.1063/1.1774590
2212 data compilation: courtesy Jianyi Jiang, Applied Superconductivity Center - NHMFL

New Hf results suggest that major improvements are still possible

- Xingchen Xu (1MOr2B-05) and co-workers at OSU,FNAL and HyperTech have shown GE's Nb-1Zr APC approach for Nb_3Sn can be adapted to wires using Nb1-Zr + SnO_2 producing high pin densities and high critical currents.
- On Monday we reported that SnO_2 may not be needed if Hf is used instead of Zr (Shreyas Balachandran's talk on Monday: 1MOr2B-06)
  - We see the potential to meet or even exceed FCC Nb_3Sn targets with or **without** SnO_2!

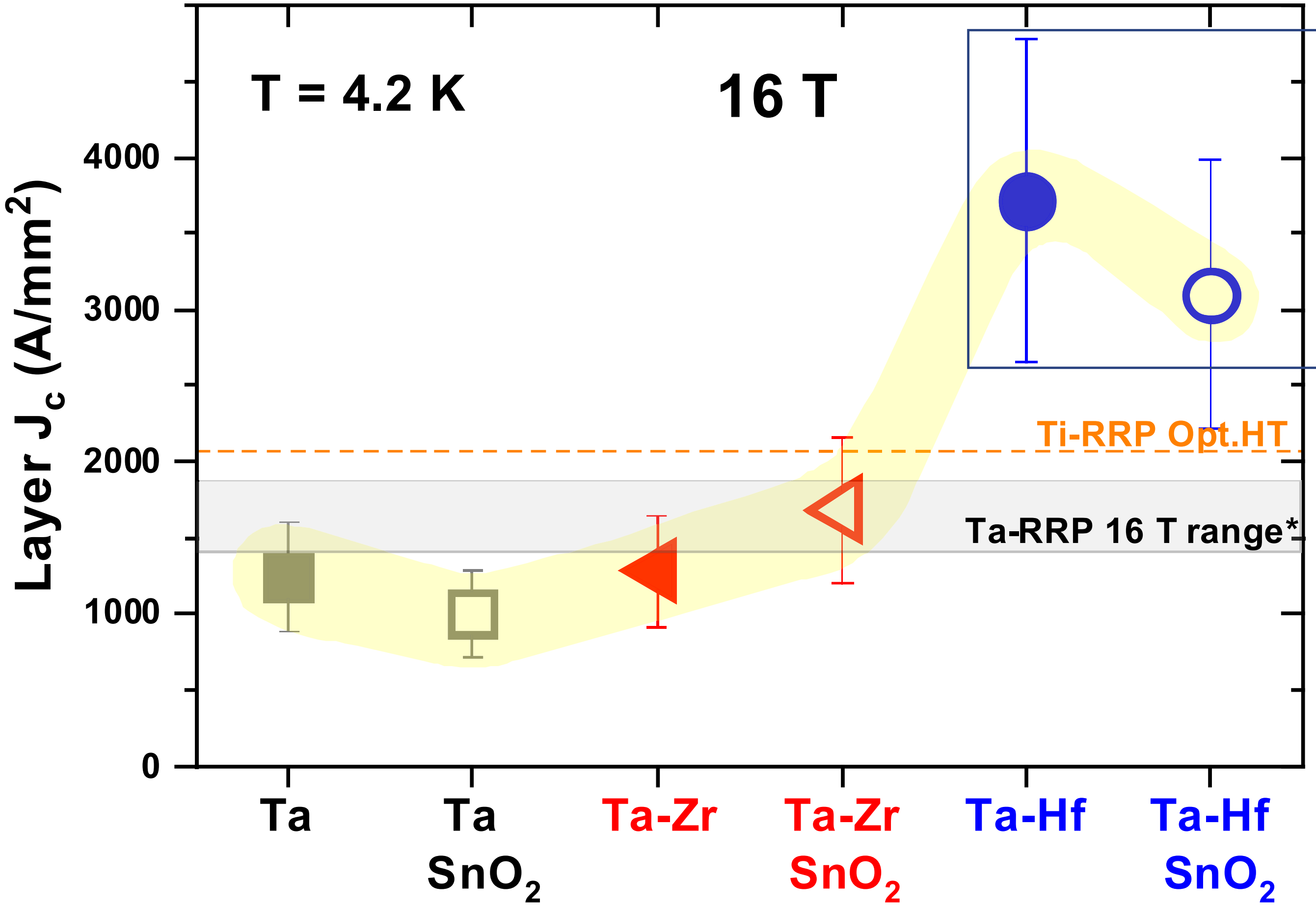

But note the error bar

http://arxiv.org/abs/1811.08867 S. Balachandran *et al.*, "Beneficial influence of Hf and Zr additions to Nb4at.%Ta on the vortex pinning of Nb_3Sn with and without an O source," *arXiv:1811.08867[cond-mat]*, Nov. 2018.

Error bar originates from inhomogeneity of prototype

- Variations in core diameters along the length and rod asymmetry illustrated here.
- Variations in Nb_3Sn layer thickness

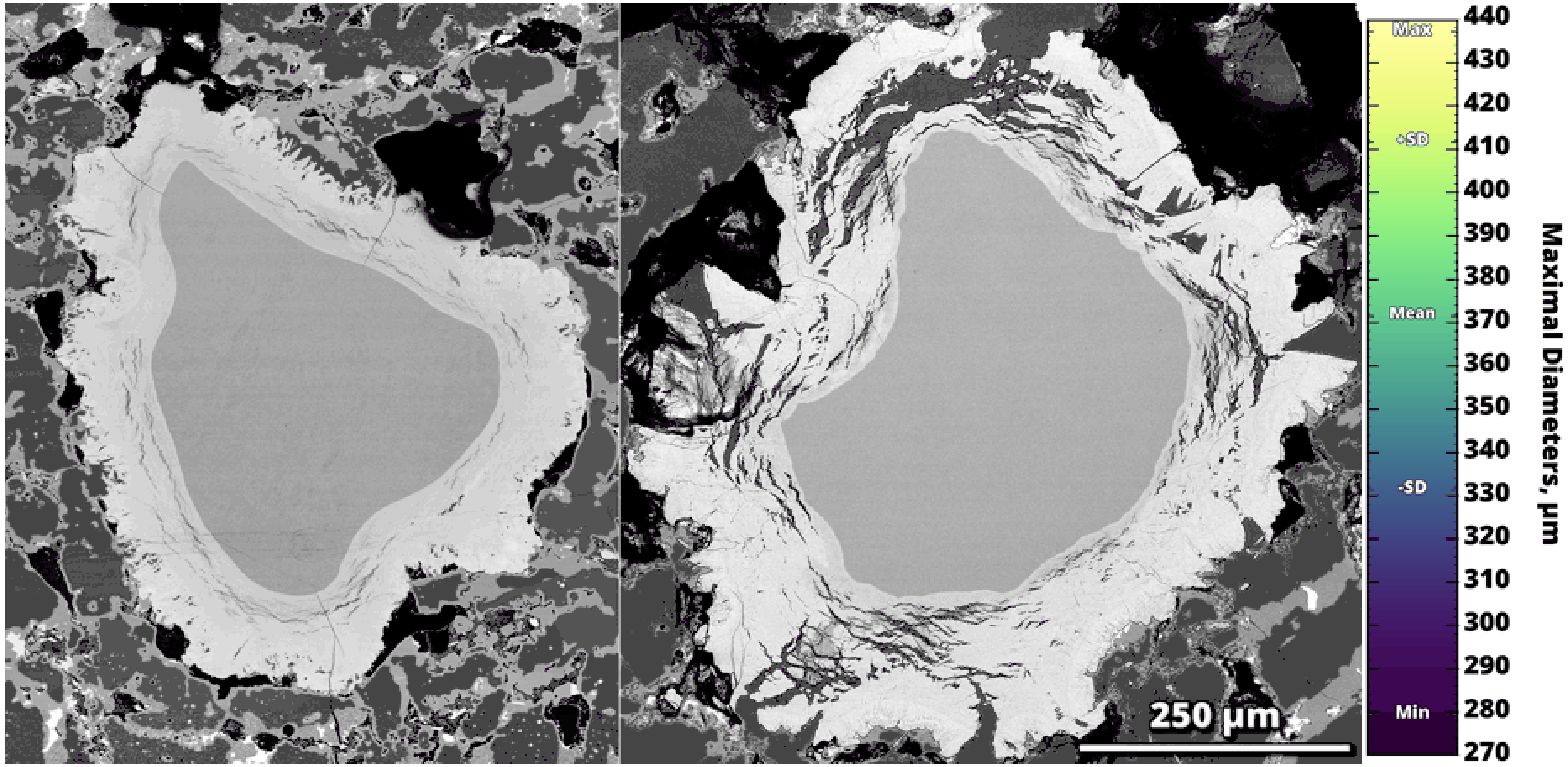

http://arxiv.org/abs/1811.08867 S. Balachandran *et al.*, "Beneficial influence of Hf and Zr additions to Nb4at.%Ta on the vortex pinning of Nb_3Sn with and without an O source," *arXiv:1811.08867[cond-mat]*, Nov. 2018.

Addressing homogeneity was a key factor in developing our understanding of Nb-47Ti

- Microscopy techniques only ever sample small fractions of the wire volume.
  - If the wire is inhomogeneous it is hard to extract quantitative data that can be compared to the properties.
  - This was a major issue for Nb-Ti because it was hard to manufacture a homogeneous alloy.

Micro-chemical inhomogeneity in a Nb-Ti alloy can be revealed a composition sensitive etch this Nb-46 weight % Ti alloy (Lee, in Wiley Encyclopedia of Electrical and Electronics Engineering, 1999).

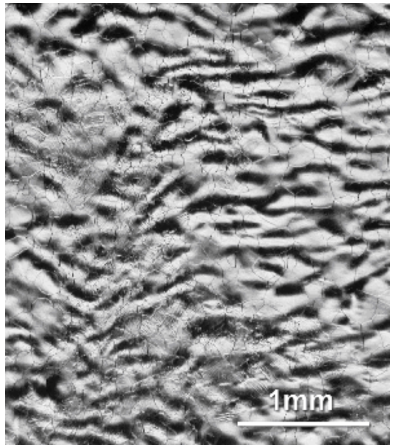

Large phase separation produces coring in alloy

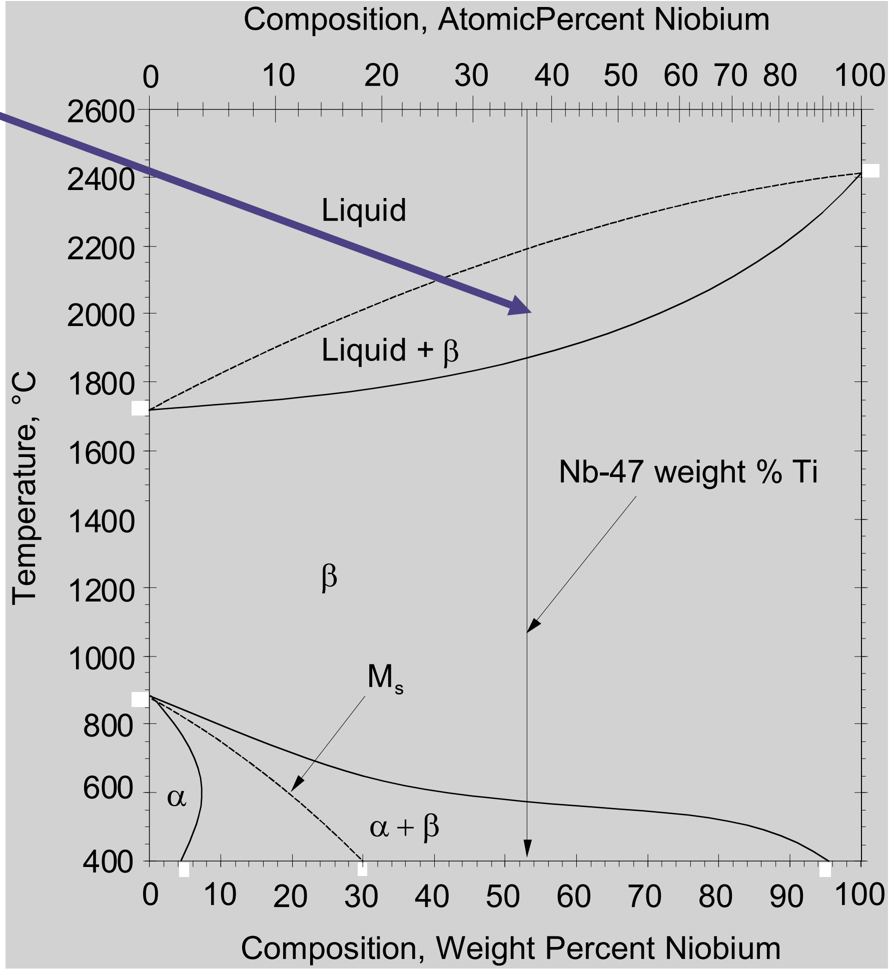

Moffat, D. L. and Kattner, U. R. "**The Stable and Metastable Ti -Nb Phase Diagrams**" *Metallurgical Transactions A* 19, no. 10 (1988): 2389–2397. doi:10.1007/BF02645466

The precipitate morphology Nb -47Ti is very sensitive to composition

- The higher the Ti content the higher the prestrain required to avoid Widmanstätten precipitation
- If the cold work prestrain is high enough and the alloy is homogeneous the microstructure will be homogeneous.

Good

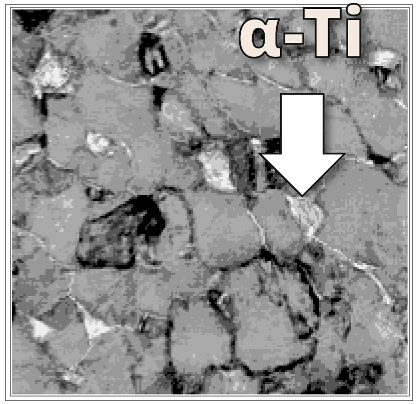

α-Ti only at grain boundary intersections – uniform size and distribution.

P. J. Lee, J. C. McKinnell, and D. C. Larbalestier, "Progress in the Understanding and Manipulation in High Jc Nb-Ti Alloy Composites," Originally published in Proc. of New Developments in Applied Superconductivity, ed. Y. Murakami, *World Scientific Press* pp. 357-362, 1989.

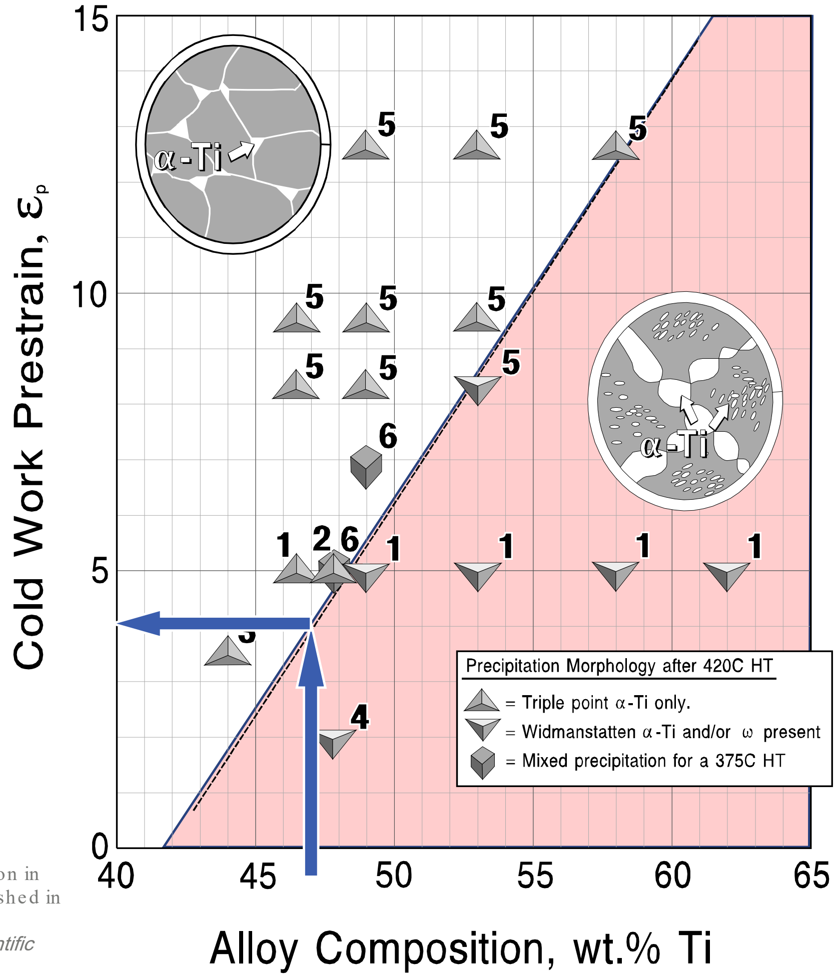

Bad

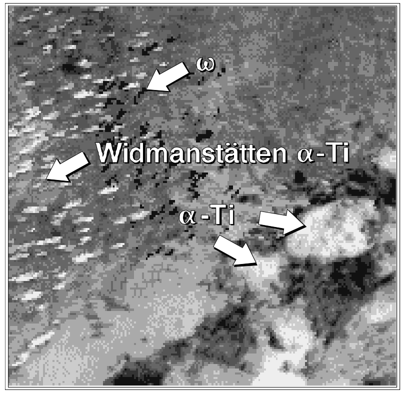

Precipitate is very inhomogeneous in size and intragranular Widmanstätten α-Ti causes severe local work hardening.

Nb-Ti: Anisotropy and Interpretation

- Before Focused Ion Beam TEM sample preparation, it was much easier to make cross-section of longitudinal lengths of Nb-Ti/Cu composites.
  - In LCS the importance of α-Ti is not apparent
- By developing new plating and electropolishing techniques it was possible to view transverse cross-sections of any size.

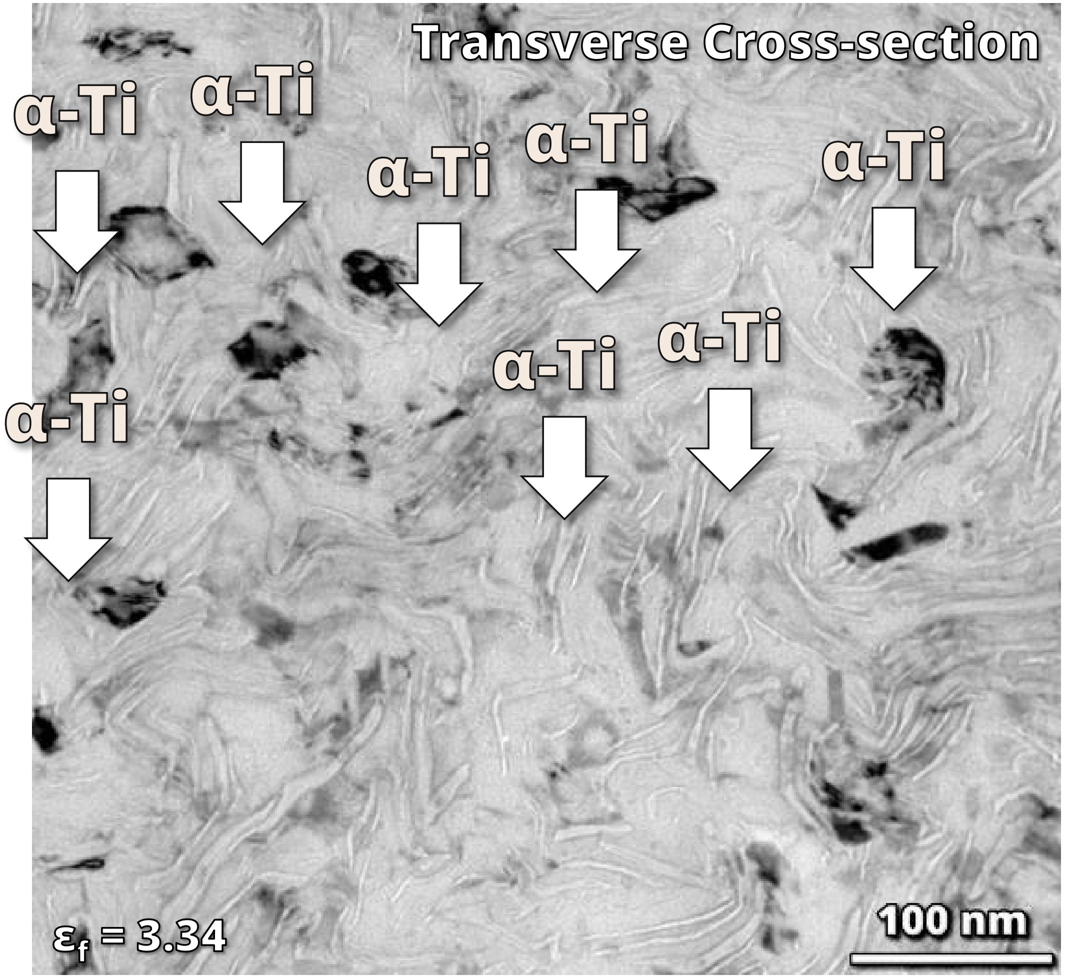

Lee and Larbalestier, Acta Met 1987 6x10h@405°C

Multiple HT and Drawing Cycles: Folded Sheets of α -Ti

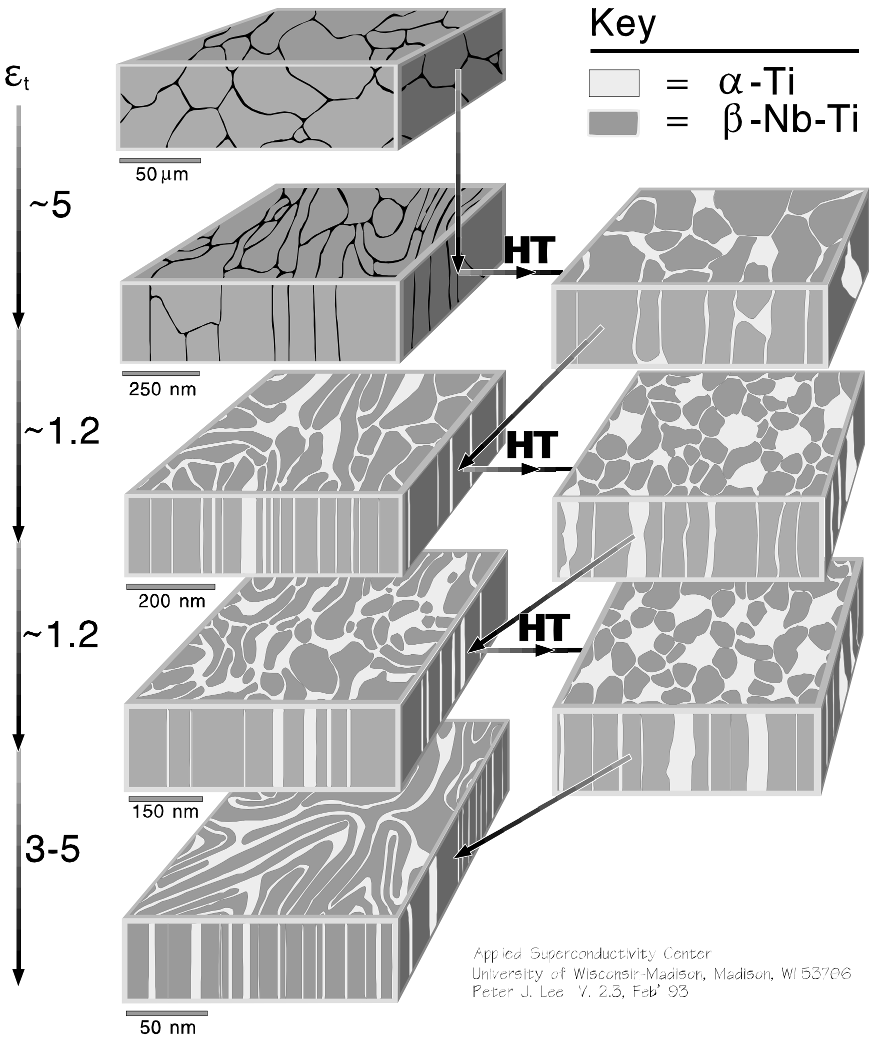

- The multiple heat treatment and drawing cycles produce a highly aspected microstructure

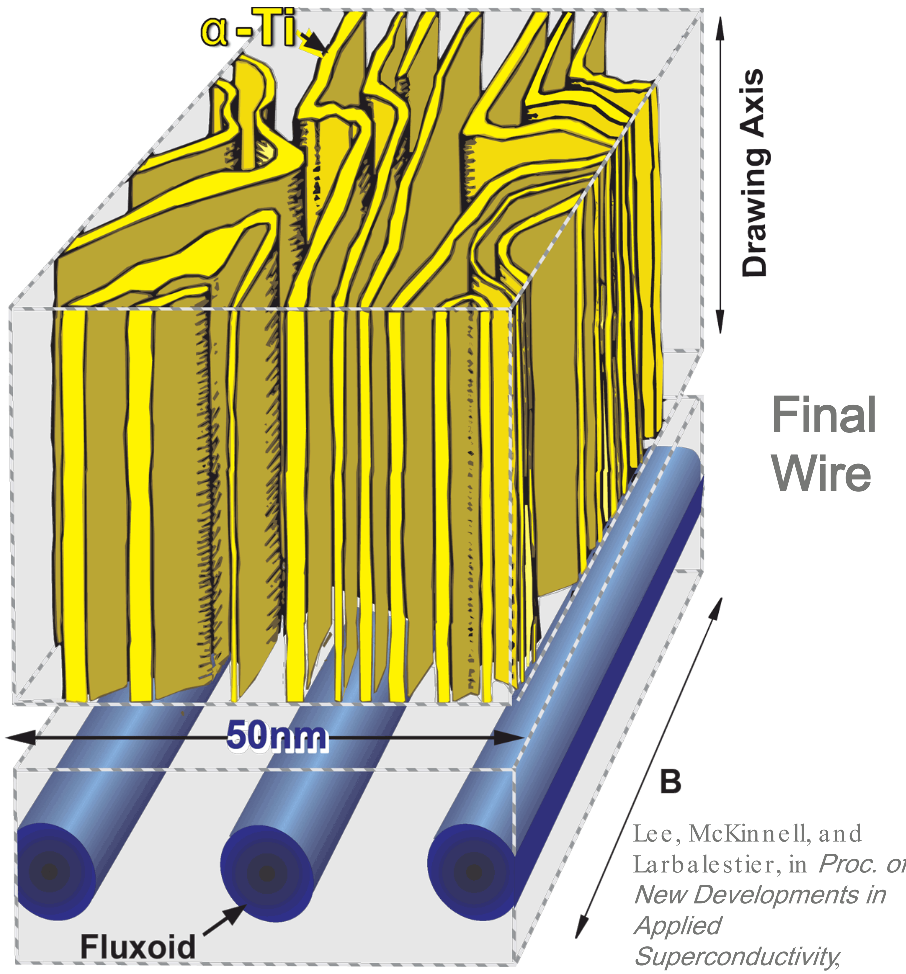

Equilibrium fluxoid spacing at 5 T, 4.2 K

Lee, McKinnell, and Larbalestier, in *Proc. of New Developments in Applied Superconductivity,* Osaka, Japan, 1989, pp. 357–362.

But Even with high quality TEM images manual quantification was required

- The complexity of the TEM contrast (diffraction contrast + atomic number contrast + foil thickness) still meant that manual measurement of the microstructures was necessary.

- However, with the excellent homogeneity of the microstructure the trends were clear and reliable correlations could be made between properties and microstructure

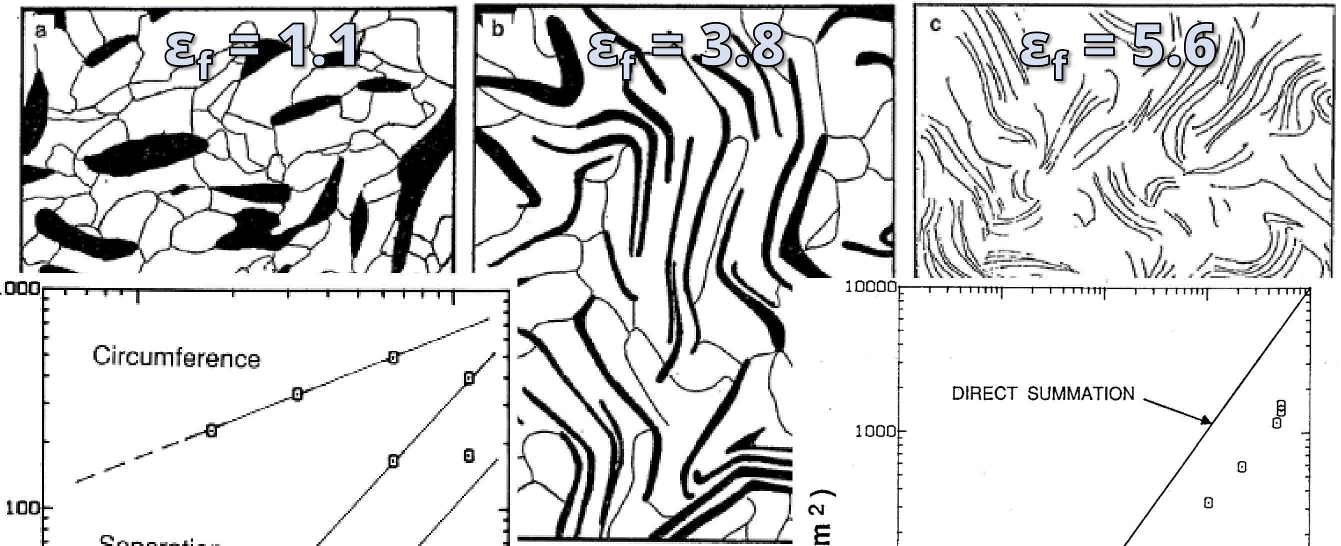

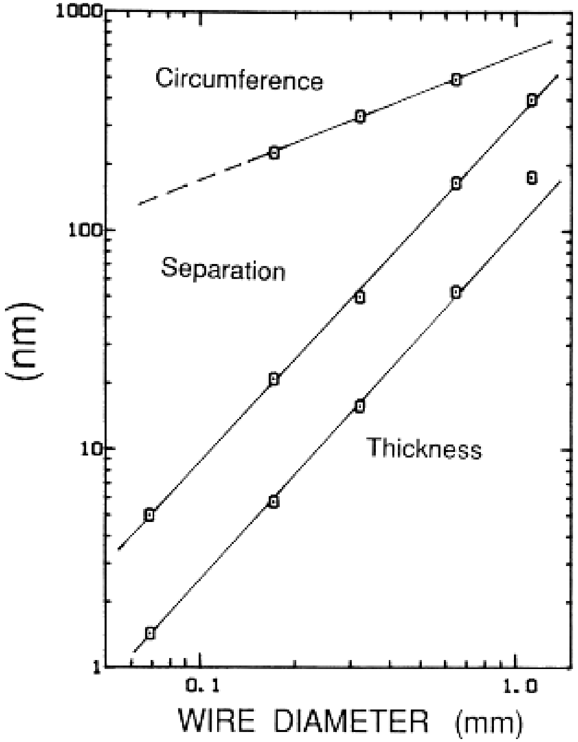

[Meingast, Lee, and Larbalestier, JAP 1989.]

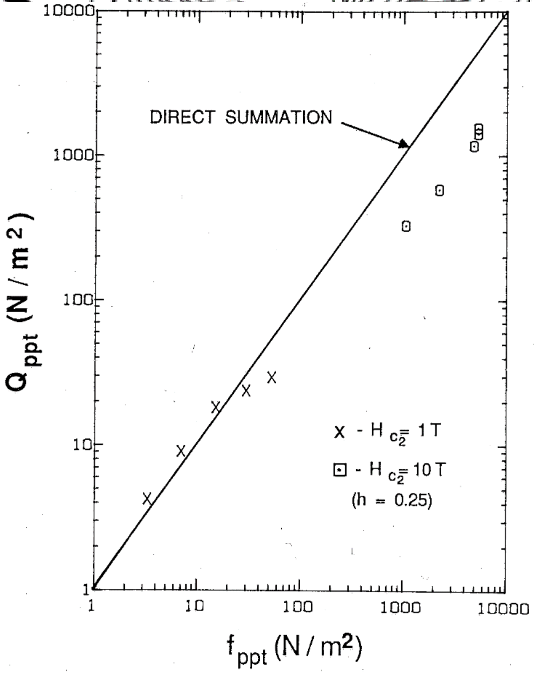

[Meingast, and Larbalestier, JAP 1989.]

Specific pinning force *(Q_{ppt})* and the calculated elementary pinning force *(f_p)*, *h* = 0.25

The digital revolution: MegaVision 1024XM – introduced 1984

- Our first digital IA system – used for all Phase II R&D SSC Nb-47Ti strand analysis
- The 1024XM had 1 Megapixel resolution, up 32 MB of real-time internal image memory and 350 Mbyte/second processing speed – which was remarkable for the time . . . so was the original MSRP for a complete system: $200,000.
- Output: Area, centroid, boundary length, form factor.

MegaVision advertising ~1984

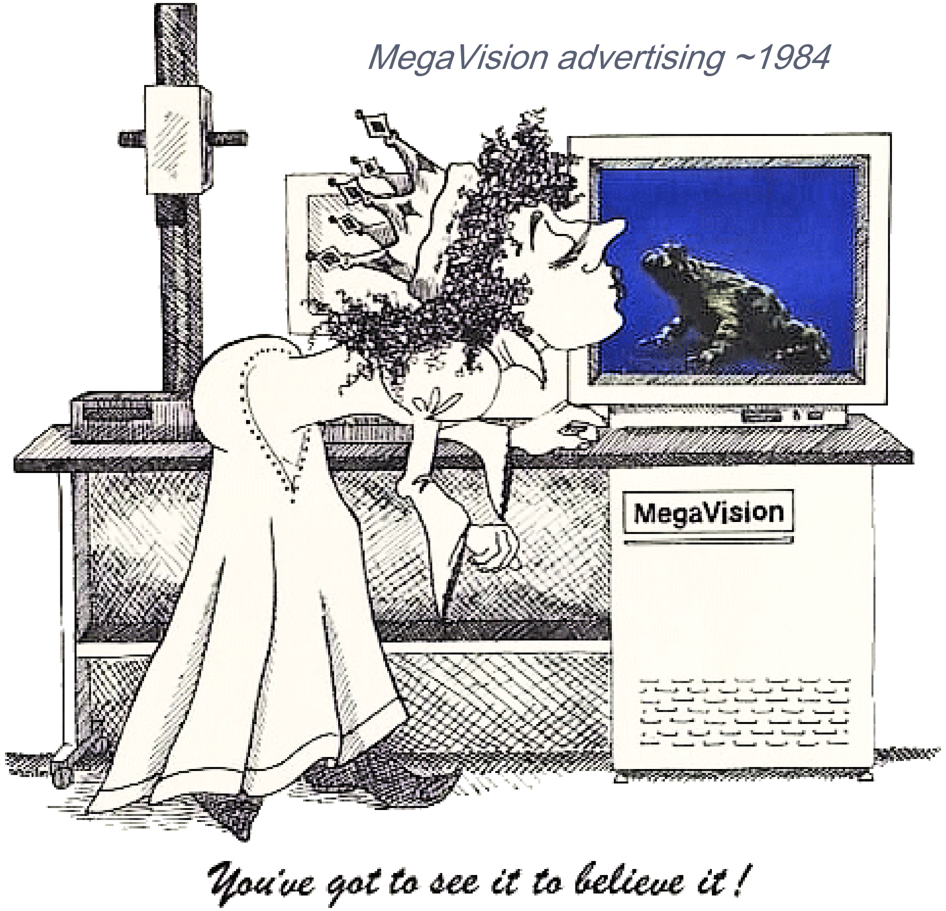

Many thanks to Dave Sutter at DOE-HEP: perhaps the first digital IA instrument for superconductivity

We the MegaVision we could combine TEM images at different tilts to remove diffraction contrast and leave mostly Z-contrast

Bright Field (SAD) TEM Images taken at different tilt angles (changing diffraction contrast)TE

Nb-47Ti $\varepsilon_f = 3$

MegaVision 1024XM processing 1994

TEM images aligned and then combined by "max intensity" – All now possible in ImageJ/Fiji for free!

Tedious but effective . . .

- The microstructure/property relationships for Nb-Ti were quantified with these relatively primitive (and expensive) digital tools combined with painstaking TEM.
- Now we can use FESEM-BSE images at most relevant magnifications.
- These later results show that critical current densities beyond the LHC are possible with new alloys and APCs

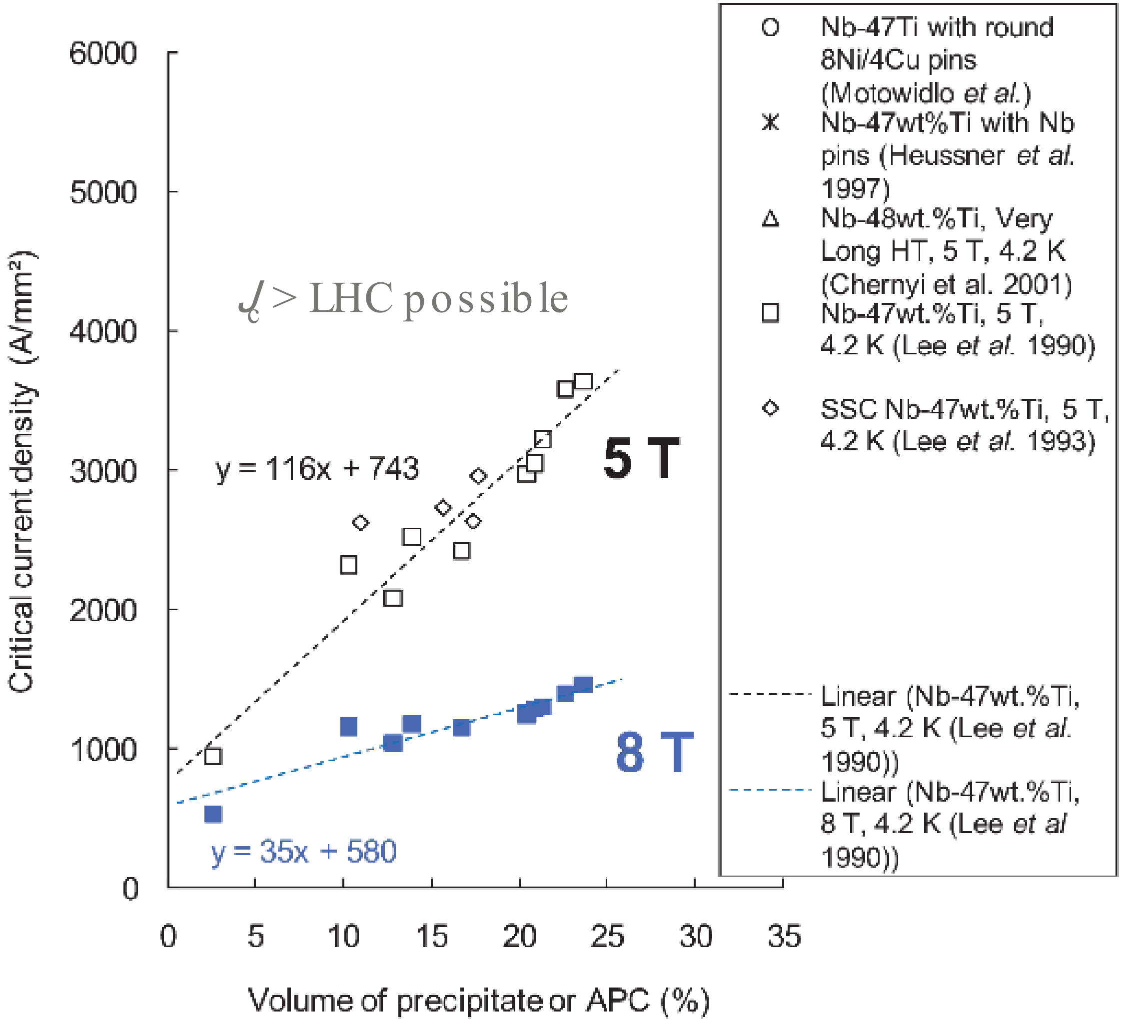

The Field Emission SEM revolution

- When we acquired our first Field Emission Scanning Electron Microscope in 1997 it made most TEM work obsolete!
  - 1 nm spatial resolution
  - High-signal low-noise Z-contrast Backscattered electron images
  - EDS and subsequently EBSD

IGC Processed Nb44-17Ta cross-section for the Fermilab IR-Quad R&D program

IGC Intermagnetics General Corporation   Fermilab

Now have intensity peaks for each phase for auto thresholding . . . But why are they not distinct?

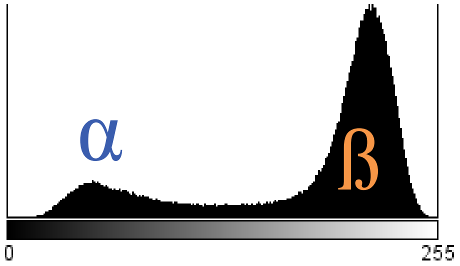

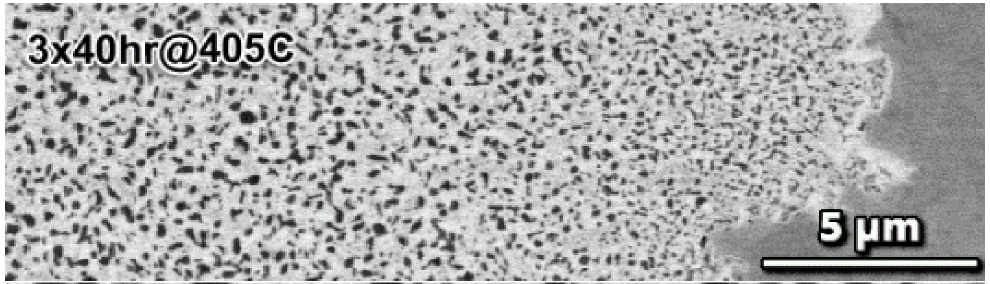

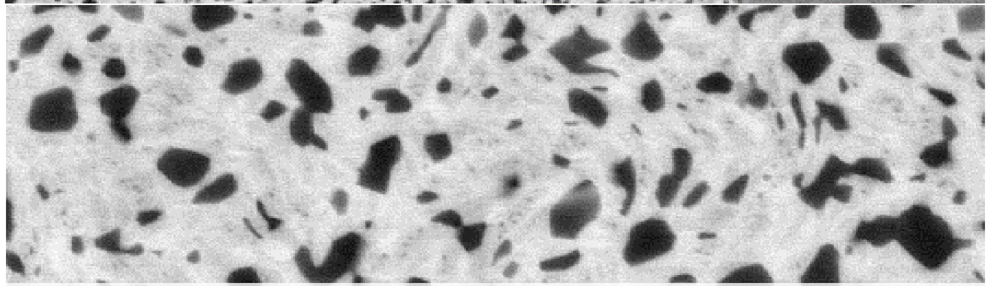

We can see the precipitation and compositional variation with great detail

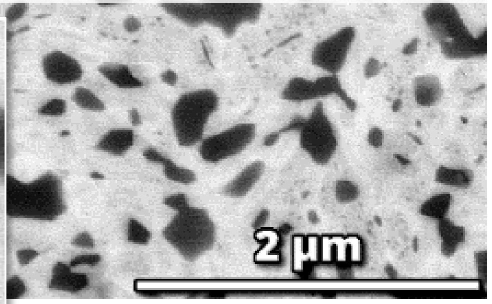

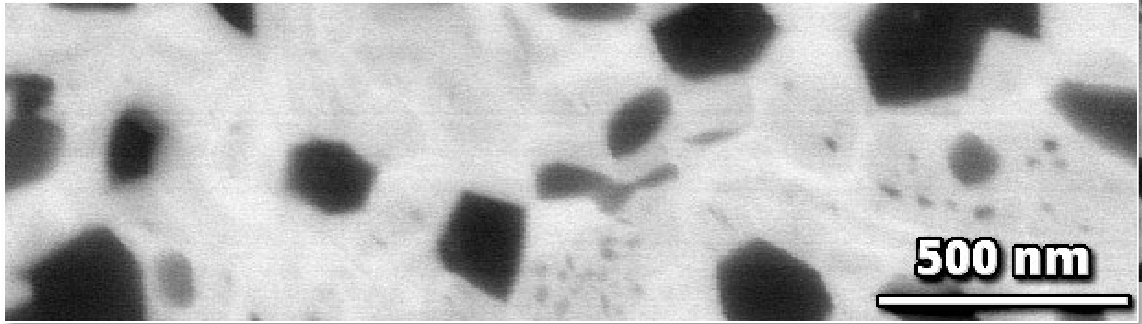

FESEM: High resolution *and* uniform image over very large areas – perfect for IA

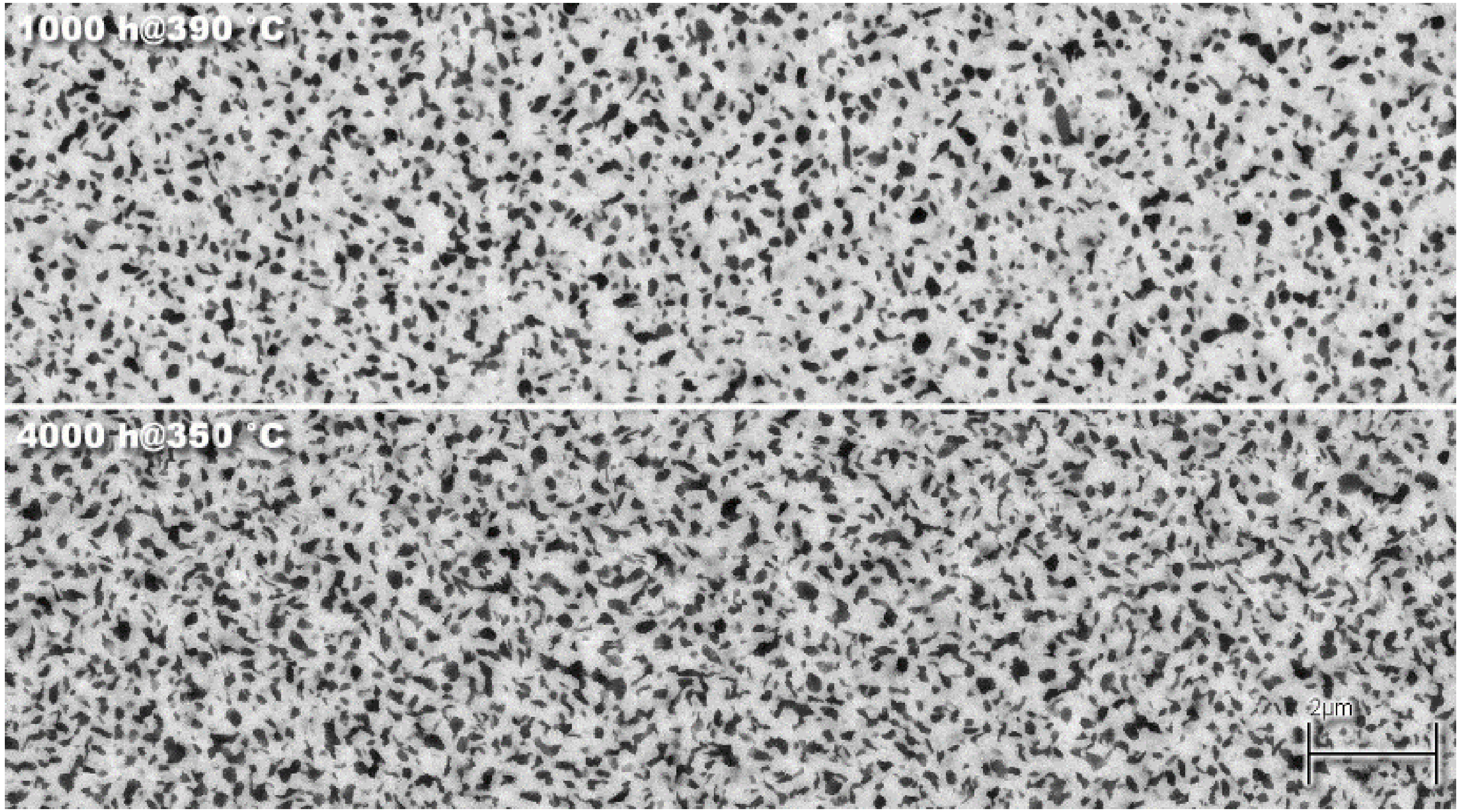

FESEM-BSE
Wire TCS

- Extended low temperature HTs produce increased a-Ti (black) volume while retaining fine scale producing world record J_c > 4000 A/mm² at 5 T, 4.2 K (Kharkov CRDF collaboration/Oleg Chernyi)

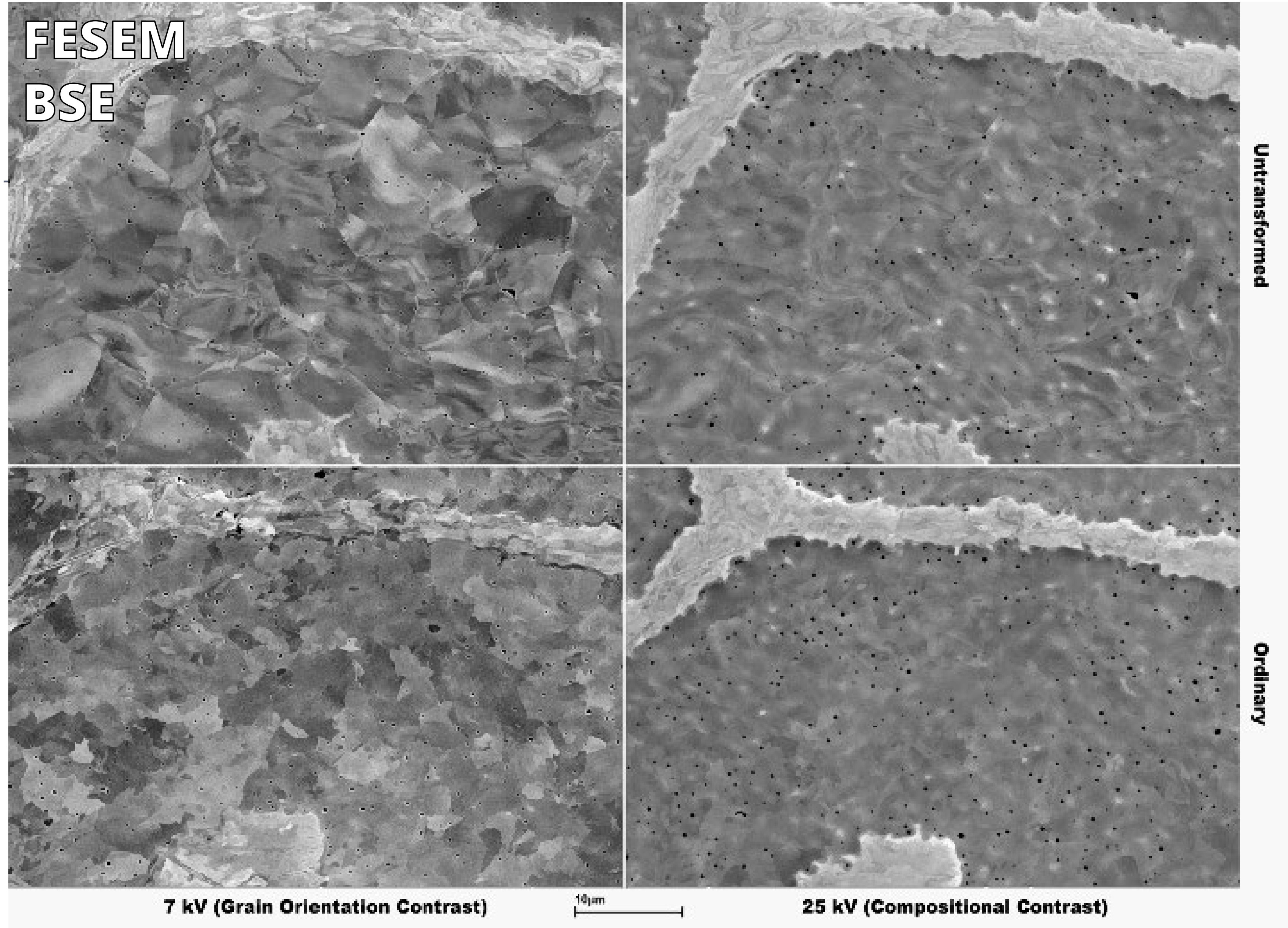

Can control BSE contrast mechanism with kV

Residual chemical inhomogeneity and large grains sizes in Nb_3Al

At 25 kV light areas=high Nb

Nb_3Al strand courtesy Takao Takeuchi, NIMS

Lee *et al.*, IEEE Transactions on Applied Superconductivity, vol. 13, no. 2, pp. 3398–3401, Jun. 2003.

Imaging at all scales possible

By using both scanning laser confocal microscopy and FESEM we have access to the full range of scale critical for Nb_3Sn cable

Sultan-tested cable courtesy of courtesy of Pierluigi Bruzzone (Plasma Physics Research Center) with agreement from the Japan Atomic Energy Agency (JAEA) and US ITER.

C. Sanabria, P. J. Lee, W. Starch, A. Devred, and D. C. Larbalestier, Superconductor Science and Technology, vol. 28, no. 12, p. 125003, Oct. 2015. http://dx.doi.org/10.1088/0953-2048/28/12/125003

ITER CSJA2 HFZ Cable

The Nb_3Sn fractures at the grain boundaries and thus we see the grain structure across the filaments.

Peter J. Lee & Carlos Sanabria

FESEM: SE

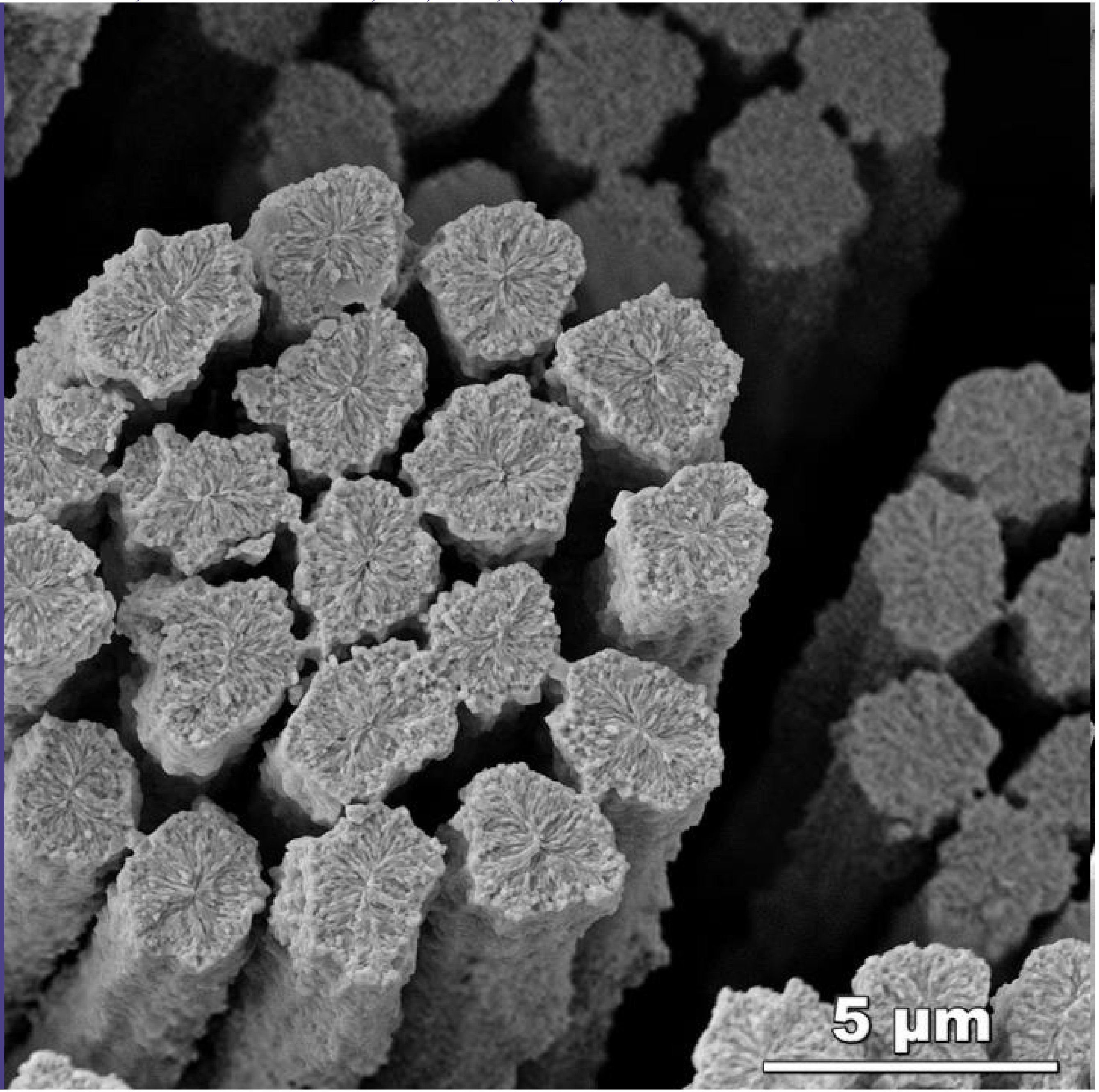

EBSD in FESEM: Deformation structures present in as-received LCLS-II SRF Nb sheets before any cavity level deformation

Shreyas Balachandran: 1LOr1A-06- ASC 2018, Seattle, Oct 28- Nov 2

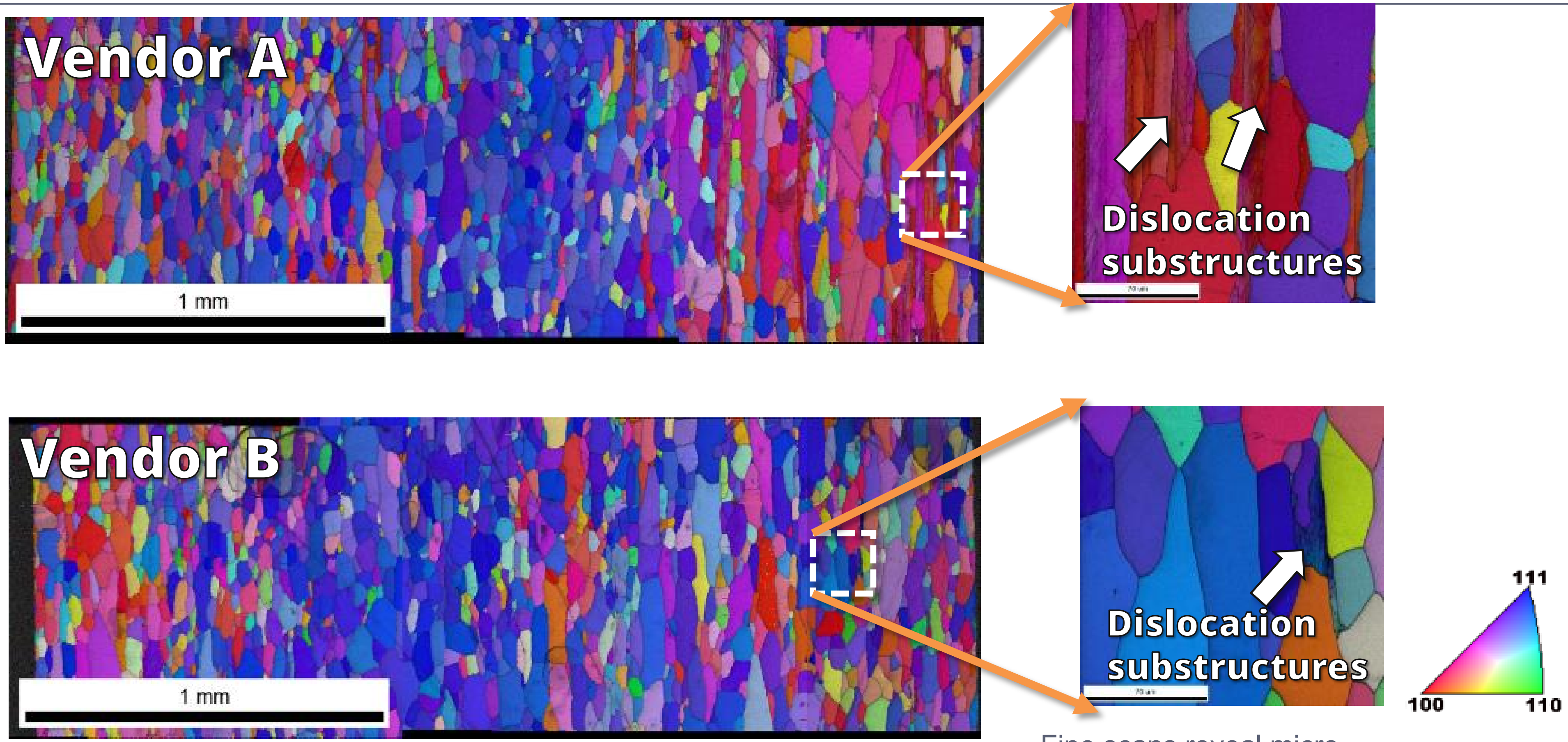

High resolution EBSD. Inverse pole figure (IPF), showing crystallographic orientations in Nb sheet material

Fine scans reveal micro-misorientations typically due to dislocation substructures

Jefferson Lab

Electron channeling contrast imaging (ECCI) of SRF Nb

Dislocations observation in bulk samples in large areas, with non-destructive sample preparation. *For SRF Nb it is really important to be able to image samples that have received exactly the same processing history as SRF cavities.*

- ECCI imaging:
  - Sample tilted and rotated to reach channeling condition (similar to TEM "two-beam" condition)
  - Dislocations appear as channeling contrast when sample is at channeling condition
- Identify dislocation (Burgers vector, slip plane) using **g** · **b** analysis

For more details about ECCI please refer to these publications:
[1]M. A. Crimp, Microscopy Research and Technique **69** (5) (2006).
[2]S. Zaefferer and N.-N. Elhami, Acta Materialia **75**, 20 (2014).

Selected area channeling patterns (SACP)

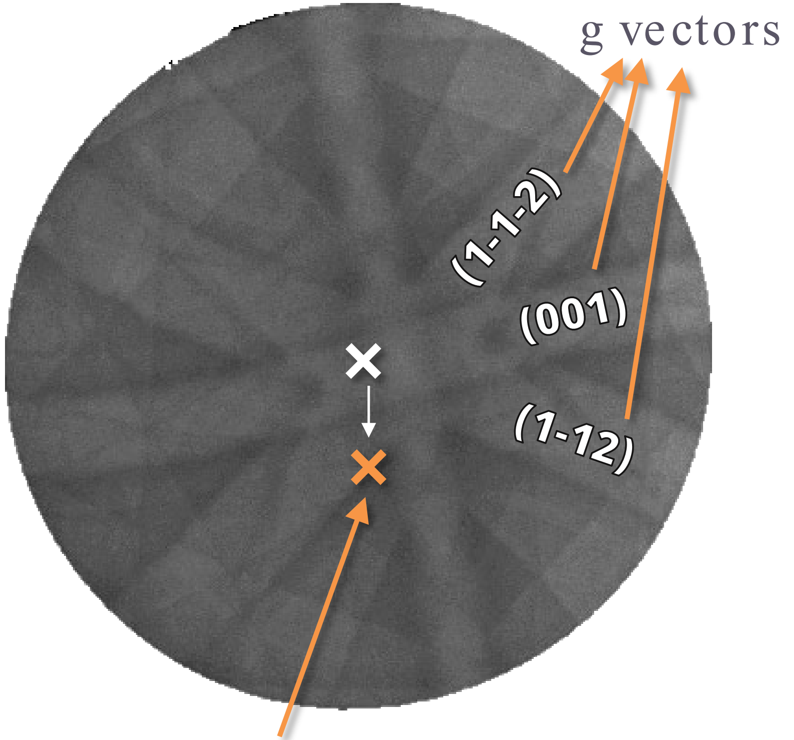

Electron beam aimed at the edge of a channeling band of g=(1-1-2) to reach a specific imaging condition

MICHIGAN STATE UNIVERSITY

Mingmin Wang
MS&T 2018

Slide courtesy of Mingmin Wang (MSU) not to be redistributed without request

Dislocation density can be estimated by manually counting number of dislocations per area from an ECCI images ($\rho \sim 10^{12}$ to $10^{13}\ m^{-2}$)

This is a lower bound of dislocation density estimation since:

- Not all dislocations are visible in a single ECCI image due to invisibility criteria
- Dislocation lines that are not perpendicular lead to underestimate of dislocation density

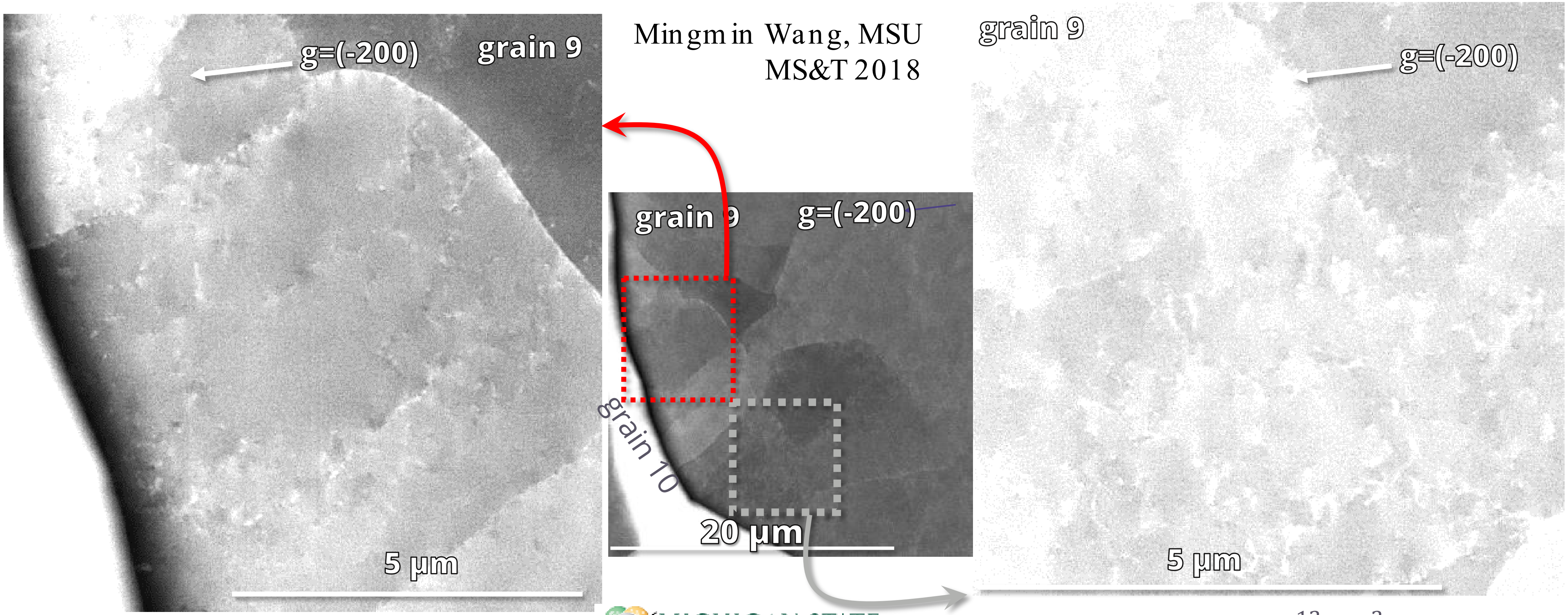

Dislocation density: $\rho = 2 \times 10^{13}$

$\rho = 4 \times 10^{12}\ m^{-2}$

MICHIGAN STATE UNIVERSITY

Micro-circuit fabrication by using Focused Ion Beam

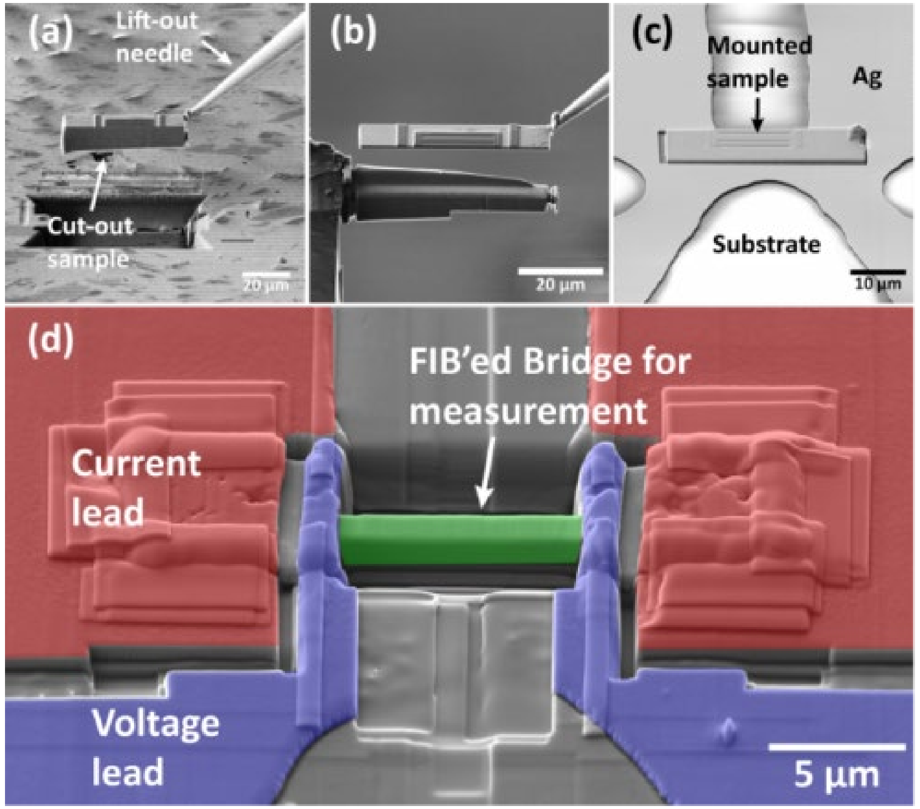

a) Cutting and lift-out.
b) Sculpting to desired shape.
c) Mounting on a Ag-patterned substrate.
d) Sculpture and deposition of metal contacts by GIS. Here the final bridge width is ~1 µm.

- Single crystal or bicrystal lamellae can be made from any form of tiny single crystal or polycrystal, even those possessing stoichiometric non-uniformity.
- Narrow FIB'ed micro-bridges drastically improve S/N
- Accurate current injection along particular crystallographic axes enables study of anisotropic behavior in any inorganic materials

Courtesy Fumitake Kametani

Reducing d_{eff} in Nb_3Sn for FCC: Example using Ta Filaments to subdivide each sub-element

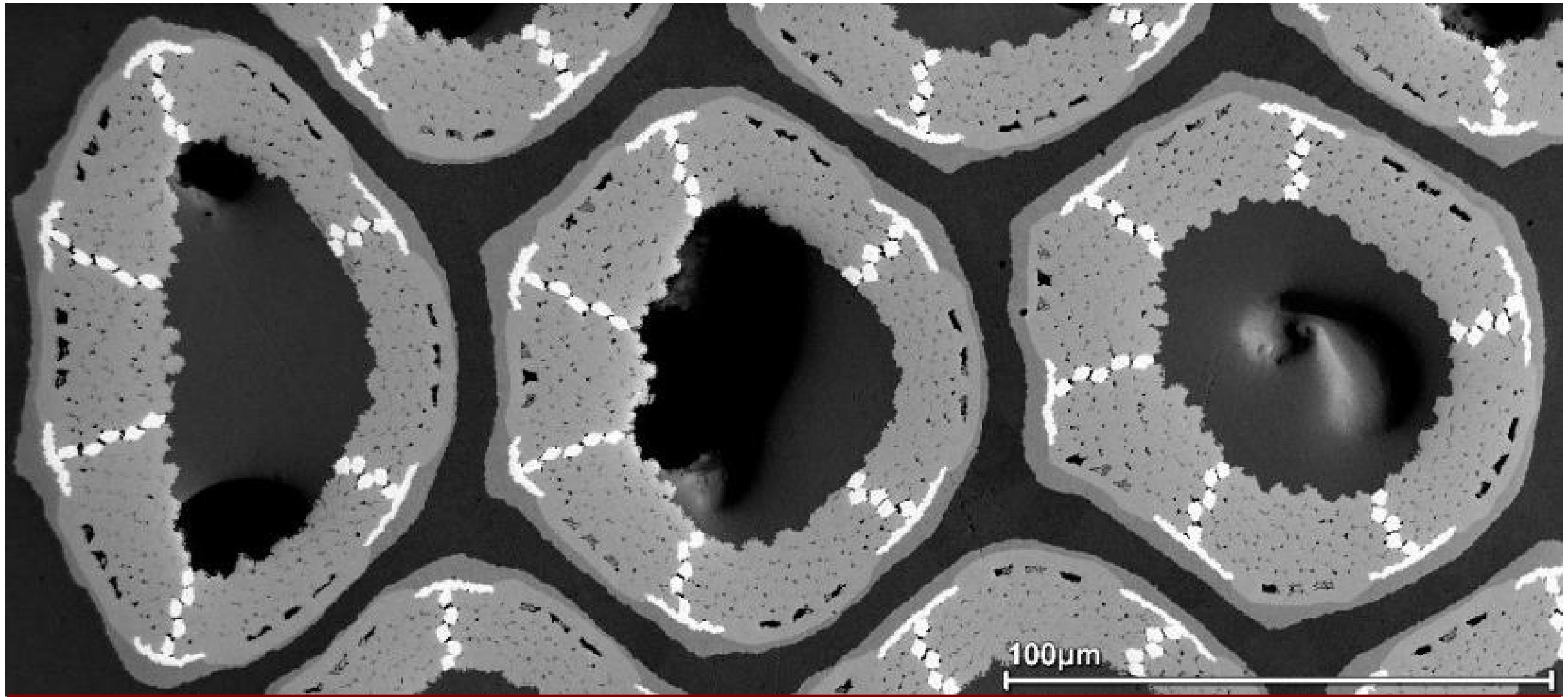

	Sub1 (outer)	Sub2 (center)	Sub3 (inner)
% of Non-Cu is Ta	4.8	5.4	5.1
% of Nb_3Sn Area lost to Dividers	9.1	10.6	9.9
% of Non-Cu is Nb_3Sn	52.7	51.3	51.6

- Probably more dividers than would be necessary:
  - 6 dividers = ~10% loss in Nb_3Sn area

OST Fabricated Strand courtesy
Seung Hong and Jeff Parrell

Sn core size was deliberately reduced in this composite

Magneto Optical Imaging: Allows Direct Imaging of B_z in Plane Above Sample

Double Faraday effect occurs in reflective mode using Bi-doped YIG indicator film with in-plane magnetization

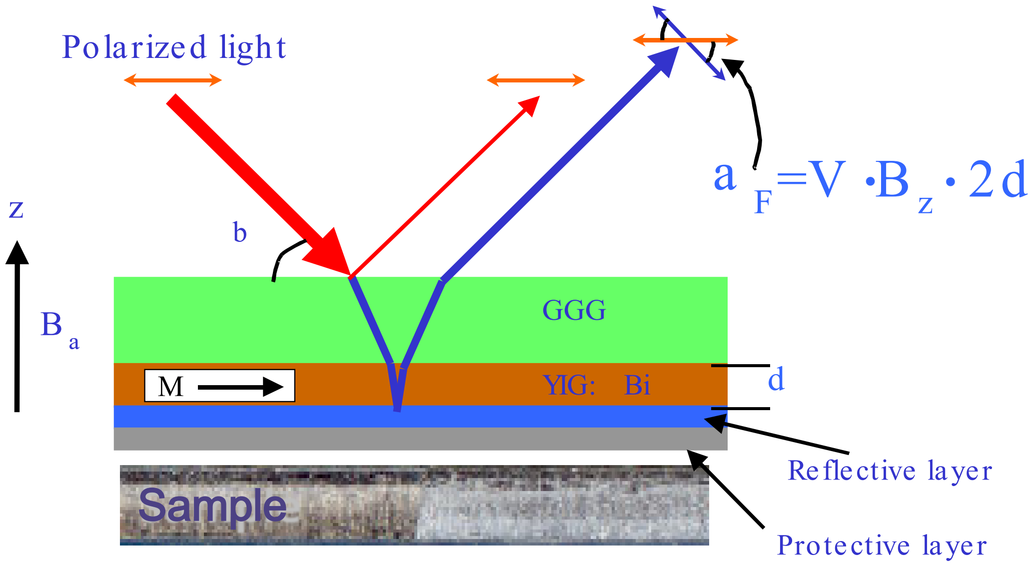

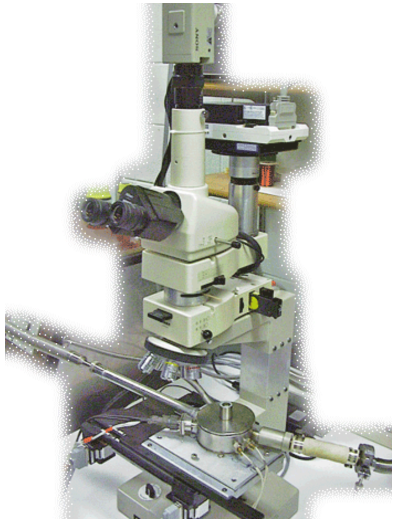

Conventional polarizing light microscope using long working distance lenses

Cryostat

Courtesy Anatolii Polyanskii

MO imaging demonstrates successful subdivision

Increasing Field

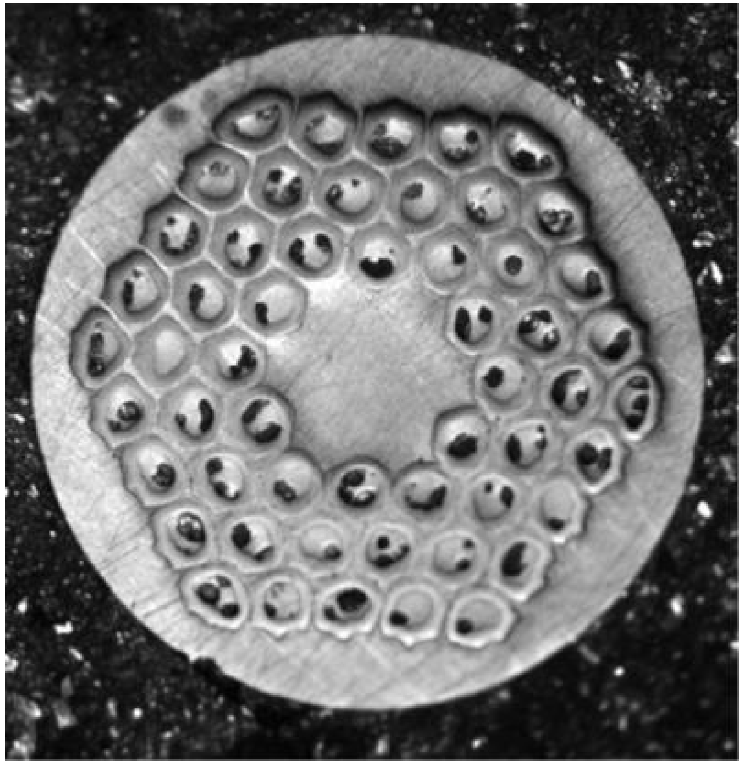

All sub-elements divided *and* cores penetrated

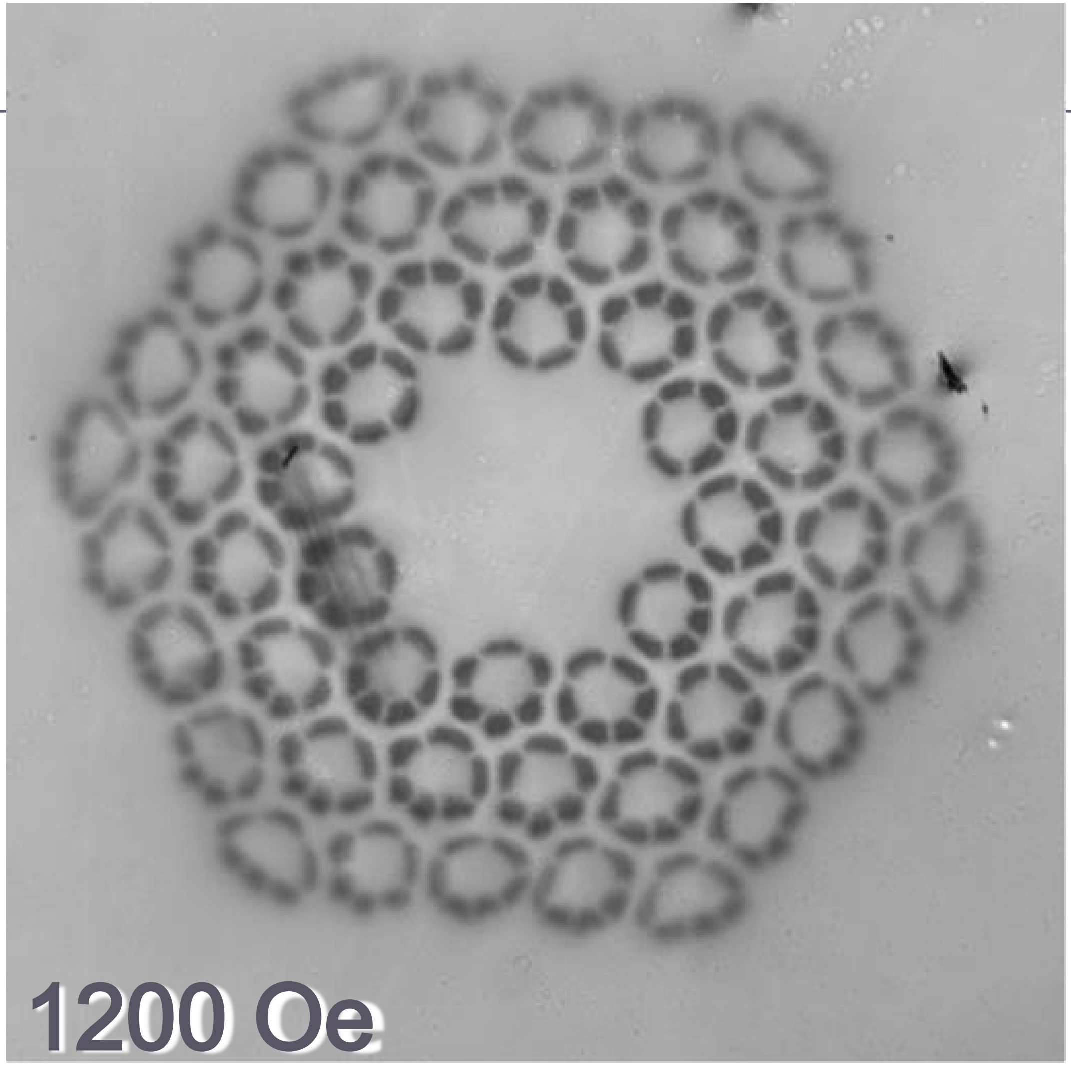

Zero Field Cooled, T=6 K

MO imaging by Anatolii Polyanskii

The computing revolution

- Needless to say the availability of increasingly powerful and more affordably computing has greatly aided the process of quantifying images.

ASC'18 Chair: Matt Jewell ~2002

Paul Allen (28) and Bill Gates (26) in Microsoft publicity photo from 1981

NIH has supported the development of free and powerful IA software

- ImageJ/Fiji is free, open source and widely supported by a very large user community!
- NIH has supported the development of a multi-platform (Linux, Mac OS X and Windows, in both 32-bit and 64-bit modes) IA tool "ImageJ" for many years to assist research in life sciences but the same tools can be used for materials science.
- A standardized open source package is now available:

"Fiji" http://fiji.sc/wiki/index.php/Fiji

Extensive tutorials are available for Fiji:

http://fiji.sc/wiki/index.php/Category:Tutorials

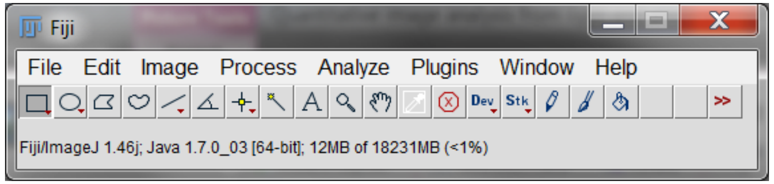

And the standard ImageJ: http://rsbweb.nih.gov/ij/docs/examples/index.html

Most importantly, the macro scripting language is designed to be easy to use and almost all actions can be recorded directly into an editable macro/script.

Very extensive list of object measurements already available and easily extendable

- The very large user community means that there are already a wide variety of feature characterizations already available.
- These measurements can be used filter and classify features.

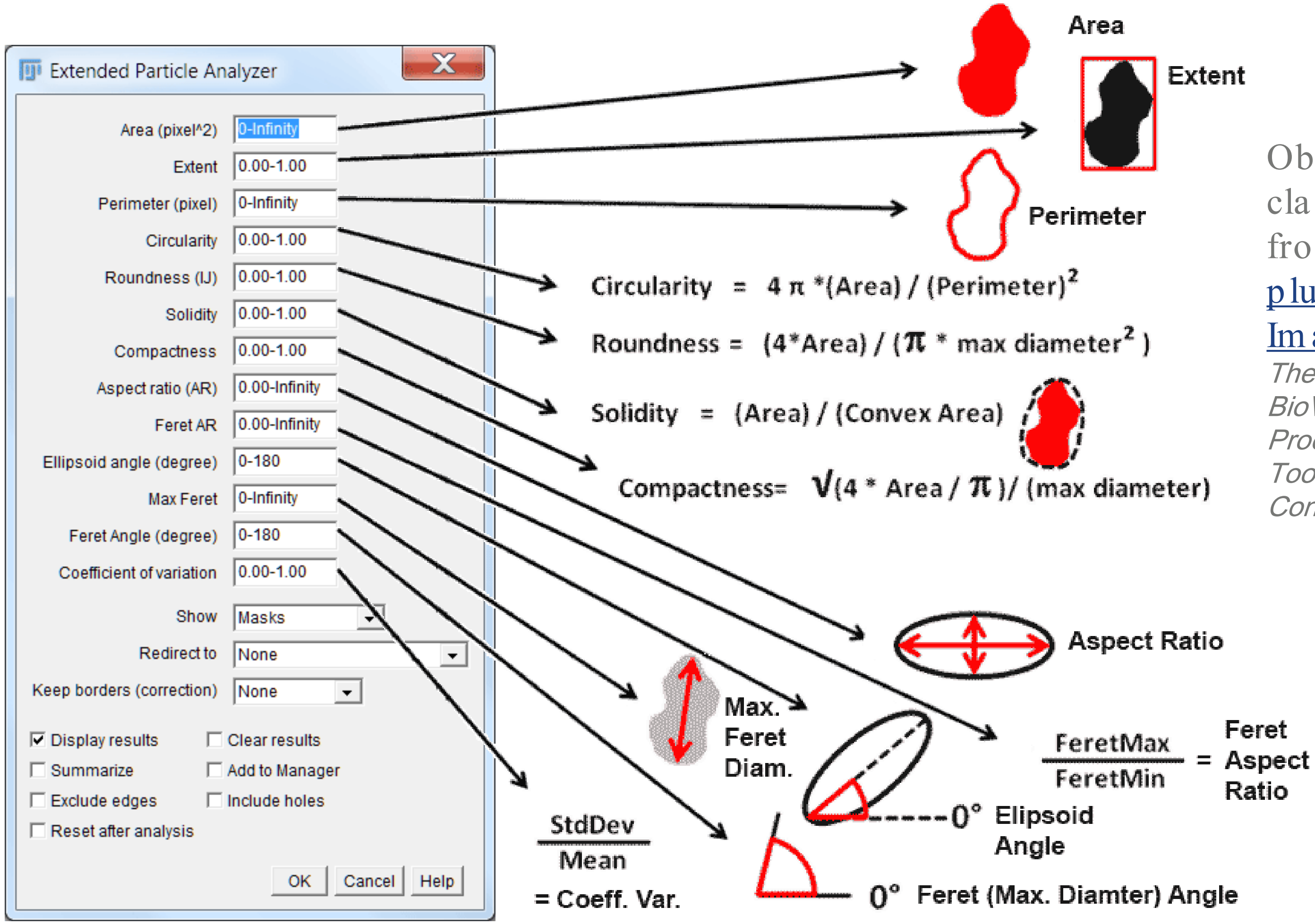

Object classifications from [BioVoxxel plugin for ImageJ/Fiji](#)

The.Brocher, 2015, BioVoxxelImage Processing and Analysis ToolboxEuBIAS Conference, 2015, Jan 5

The Power of ImageJ/Fiji Macros

- By using macros you can apply a uniform and complex processing and analysis process to multiple images.

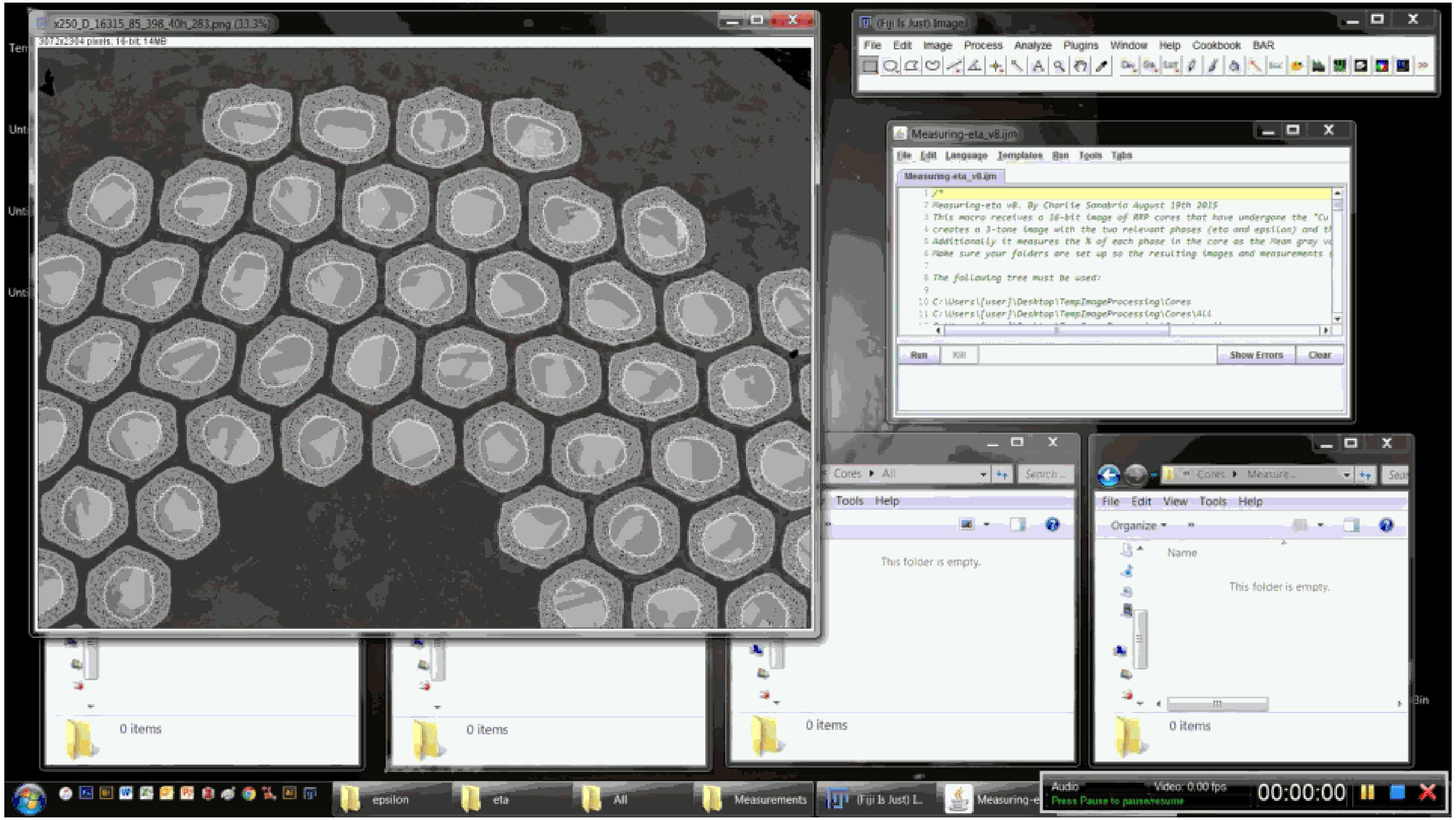

This macro by Charlie Sanabria analyses the ε to η ratio in RRP internal Sn Nb_3Sn strand.

ASC/NHMFL developed ImageJ macros available

http://fs.magnet.fsu.edu/~lee/asc/ImageJUtilities/ASC_ImageJ_Utils.html

The variation in thickness in the Nb diffusion barrier along its length is measured for outward diffusion along its length.
The darker the line the shorter the outward diffusion path (note, however the large grains - for grain boundary diffusion we would need a different analysis).

Minimum (and Maximum) — Distance Measurements

- Many microstructural features relevant to superconducting properties change in size, distribution, morphology and chemistry with distance from an interface (e.g. relative to a diffusion source or a diffusion barrier).
- This macro adds the minimum distance between the centroid of a set of analyzed objects and a reference set of points to the ImageJ results table.
  - This data can then used to provide position normalized quantification of microstructures, microchemistry
  - And even images (Next Slide)
- Examples:
  - Minimum and Maximum distance to reference set.
    Minimum distance to center (based on mean of coordinates) of reference.
    Angular orientation of minimum distance direction (degrees)

Positional Normalization to Interface/Feature

Here we have a high resolution atomic number (z) sensitive FESEM BSE image of a Nb_3Sn filament.
The image is noisy, there is some dirt on the surface and there is some orientation contrast . . .
but it will do! *Mostly Intensity ∝ Z*

1. We know the x,y coordinates of each pixel in the filament.
2. In ImageJ we can generate an outline of the filament and output those x,y co-ordinates.
3. We can use the ImageJ/Fiji macro to calculate the distance of each pixel (z value) from the interface.

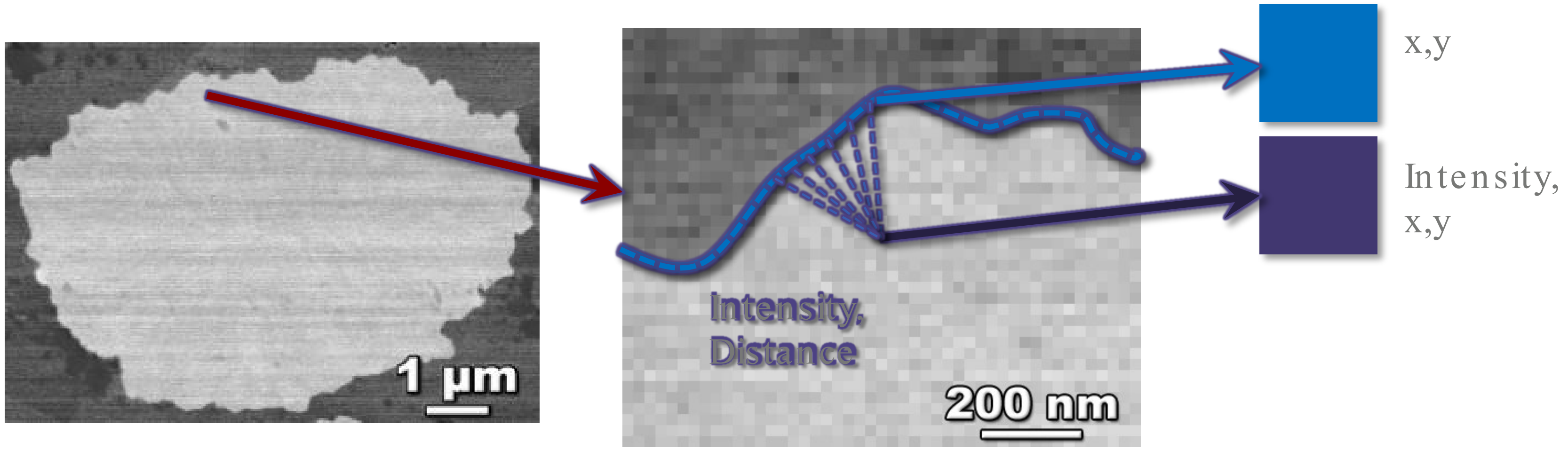

Sn content gradient in diffusion barrier wrap

- Cu layer is added between barrier wraps to enhance bonding and to allow flux penetration and reduce hysteretic loss.
- Z-contrast analysis shows that Sn diffuses along the entire length as shown by Z-contrast gradient
- Gradient inside barrier suggests a Sn depletion gradient towards wrap.

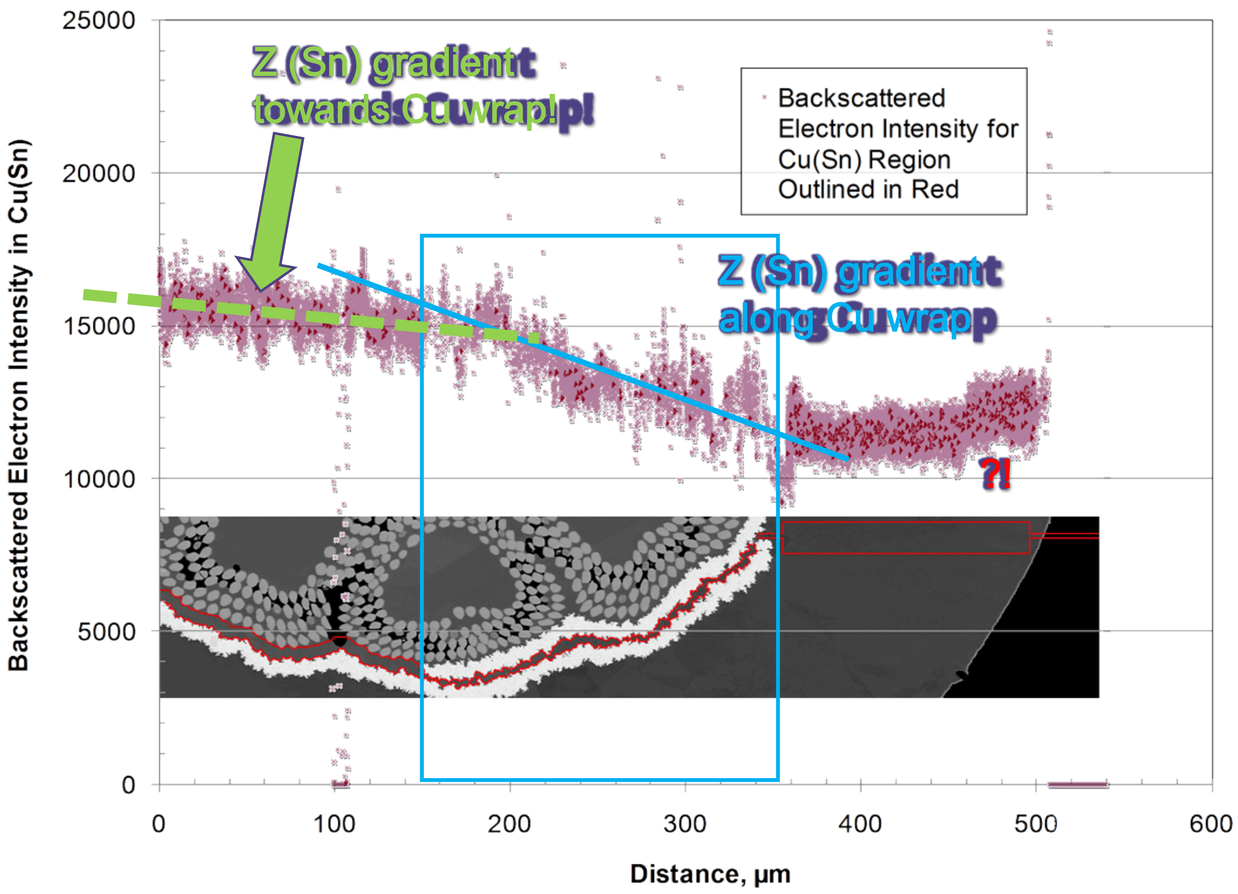

SRF Nb: Impact of N doping on hydride precipitation

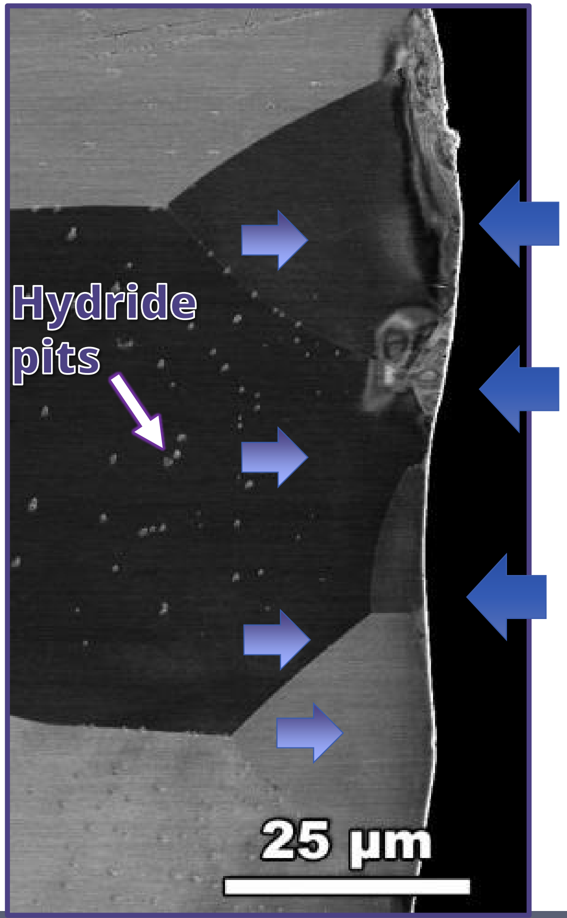

See: P. Garg et al., "Revealing the role of nitrogen on hydride nucleation and stability in pure niobium using first-principles calculations," *Supercond. Sci. Technol.* vol. 31, no. 11, p. 115007, Oct. 2018.

N diffusion into Nb

From Shreyas Balachandran

Lower hydride density from the surface boundary in N doped Nb.

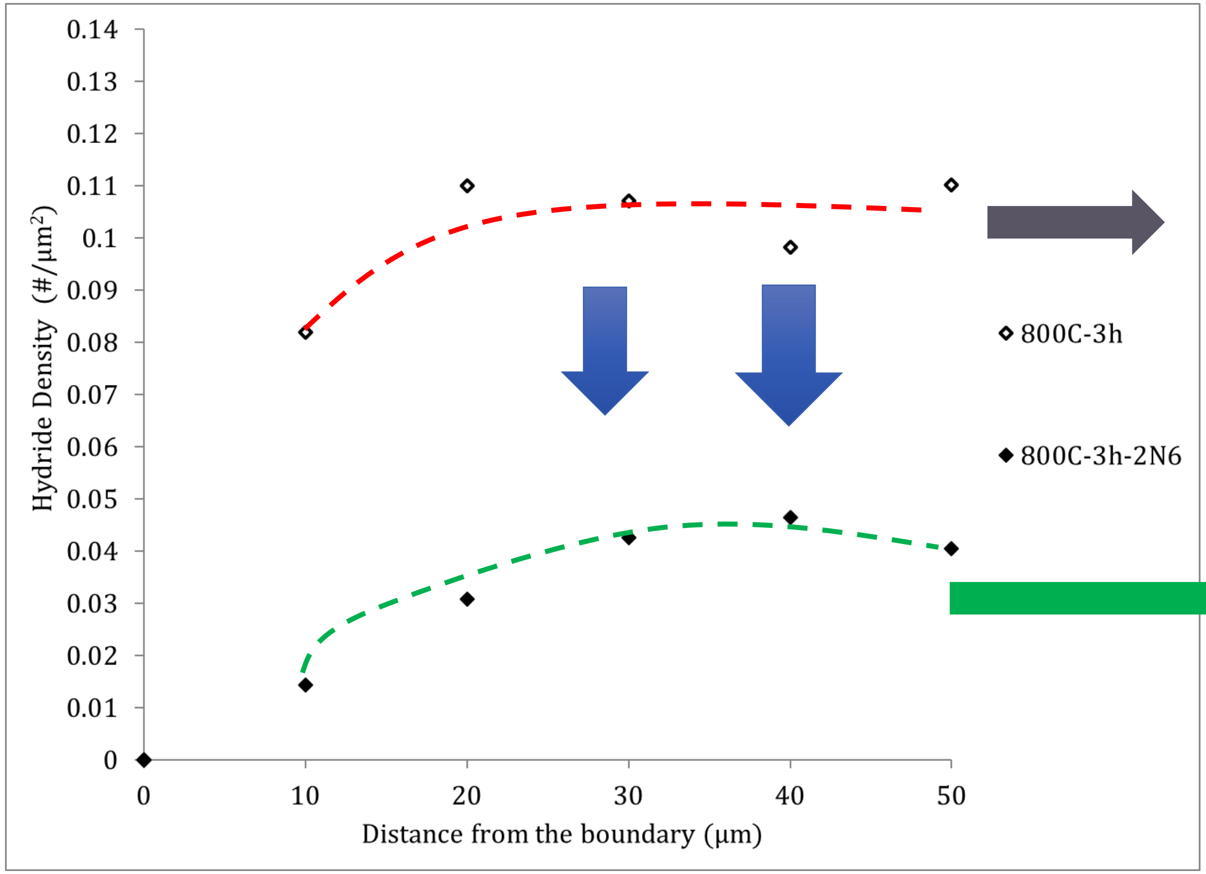

Image J/Fiji macro to calculate the distance between hydride pit and boundary

See: P. Garg et al., "Revealing the role of nitrogen on hydride nucleation and stability in pure niobium using first-principles calculations," *Supercond. Sci. Technol.* vol. 31, no. 11, p. 115007, Oct. 2018.

From Shreyas Balachandran

Layer Thickness

- These macros measure the minimum wall thickness of open or closed objects from the perspective of each pixel on the interior or exterior of a wall.
  - Choosing the direction here is important
- If the wall is broken (incomplete) there is a version that uses an interior object to define the open and closed regions (this also allows a measurement of the percent of wall that is open).
- A detailed explanation of the two macros is provided at the web site.

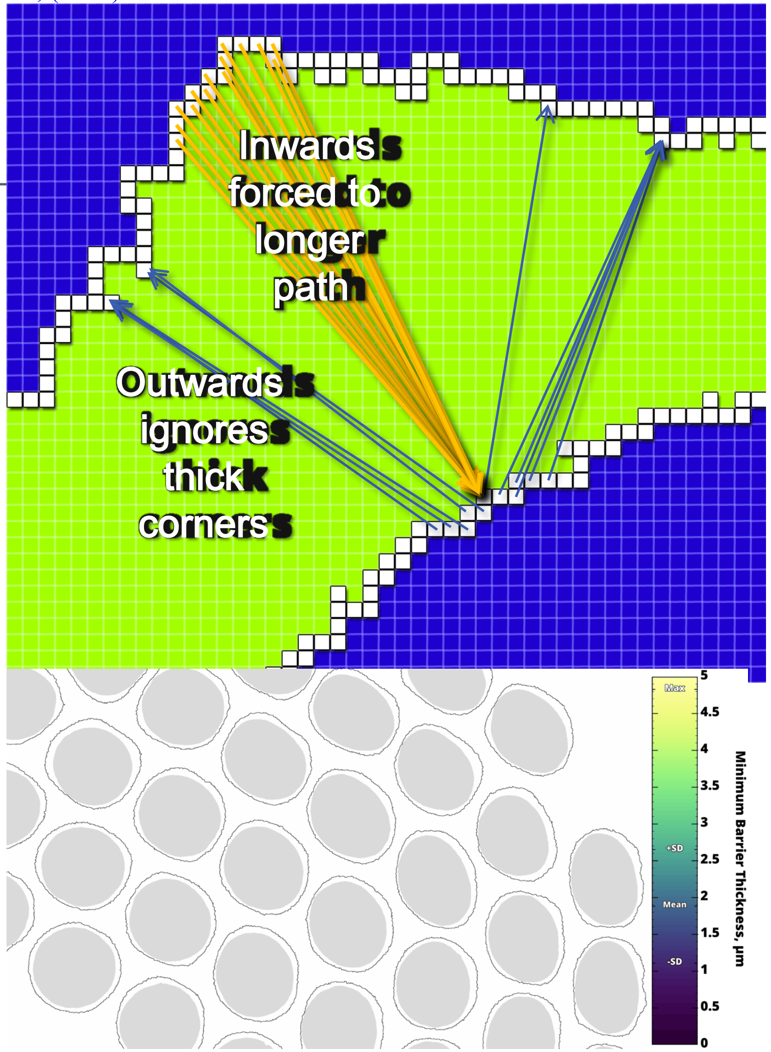

Unreacted barrier thickness in Bruker PIT strand fabricated for CERN
Image Analysis by Chris Segal (now at CERN).

Color By Feature

- The BAR ("Broadly Applicable Routines") collection maintained by Tiago Ferreira has numerous features but our favorite is the ROI (region of interest) color coder:
  - Colors each analyzed object with a color based on any set of feature values.
- We have extended the formatting options of this macro to provide more flexibility; the number of options might look intimidating but the defaults should be reasonable choices and scale with image size.

Linear or log stats can be displayed

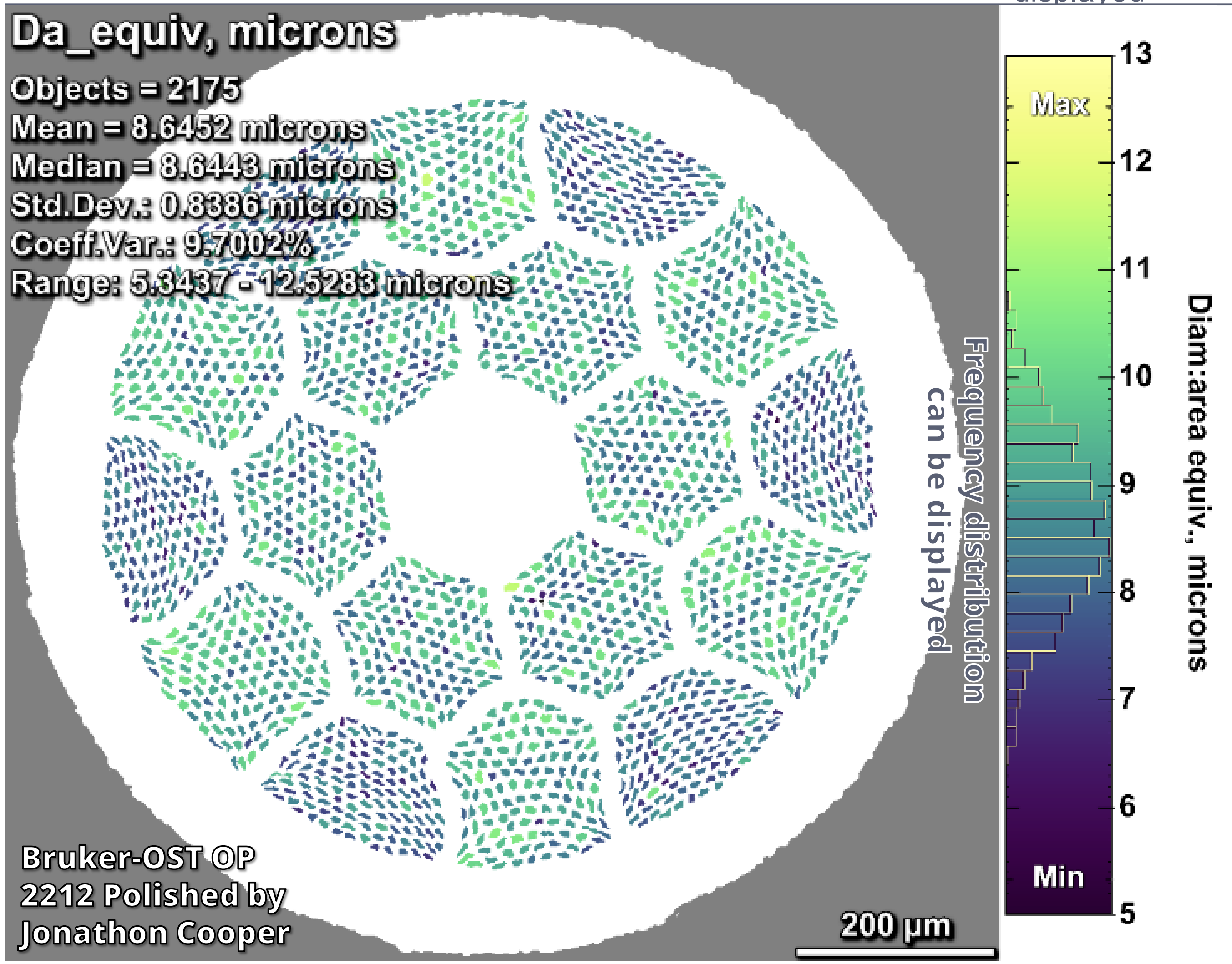

Touch Count and Proximity

- The minimum separation of objects can be measured
  - The number of objects touching each other can be counted
  - The number of adjacent objects within a set distance can be counted
- The nearest neighbor distance can be calculated

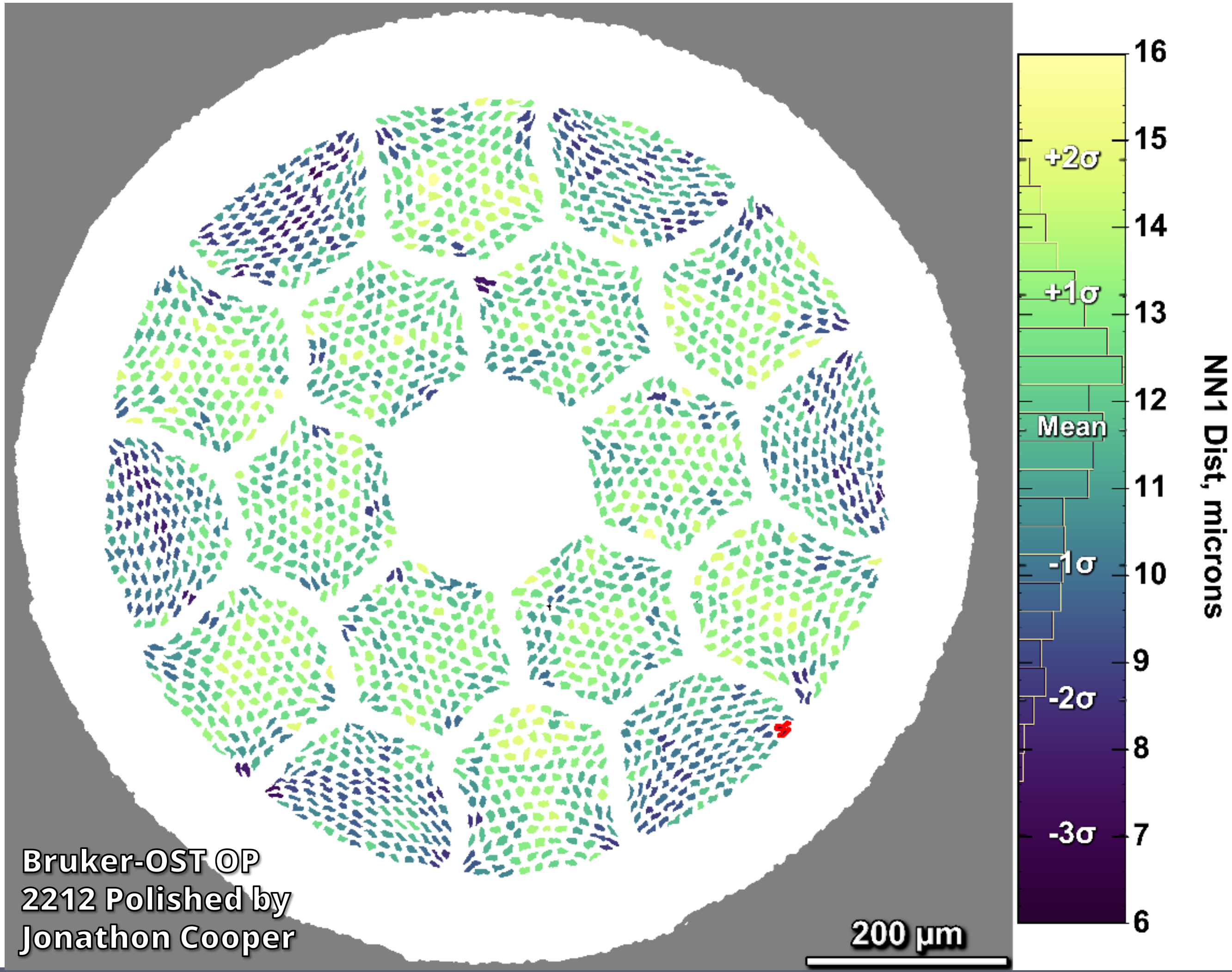

ITER CSIO1: SC vs SC+Cu

Iter EUTF5 CICC after testing in Sultan

Sanabria et al. SuST 2015

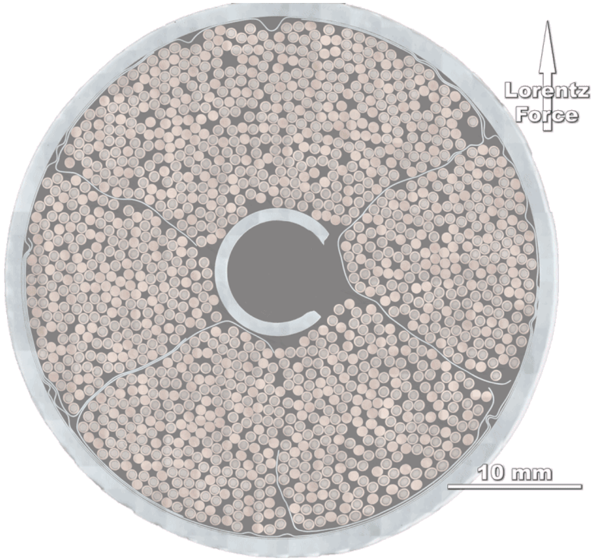

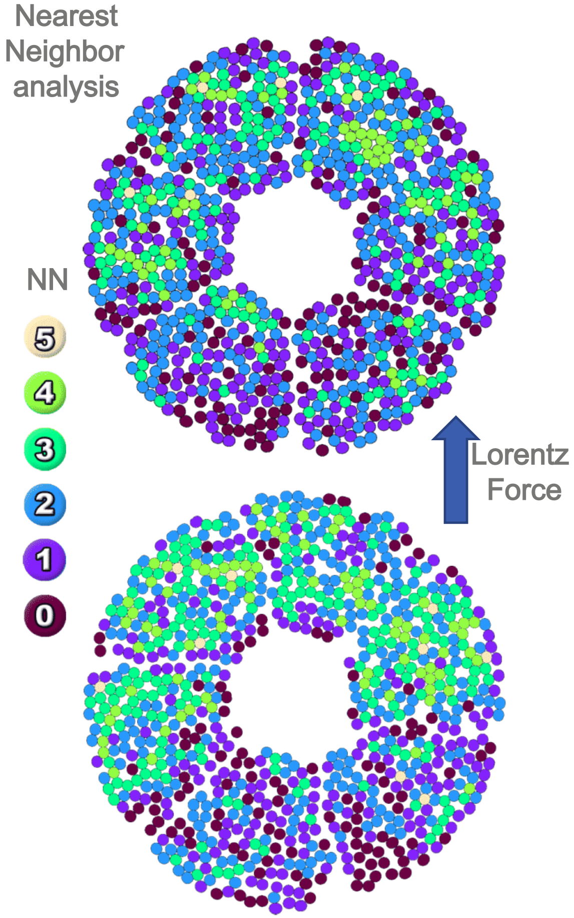

CSIO1-1 without copper strands (reduce current/strand also 20% more SC)

CSIO1-2 with copper strands (typical design).

SULTAN-tested High Field Zone

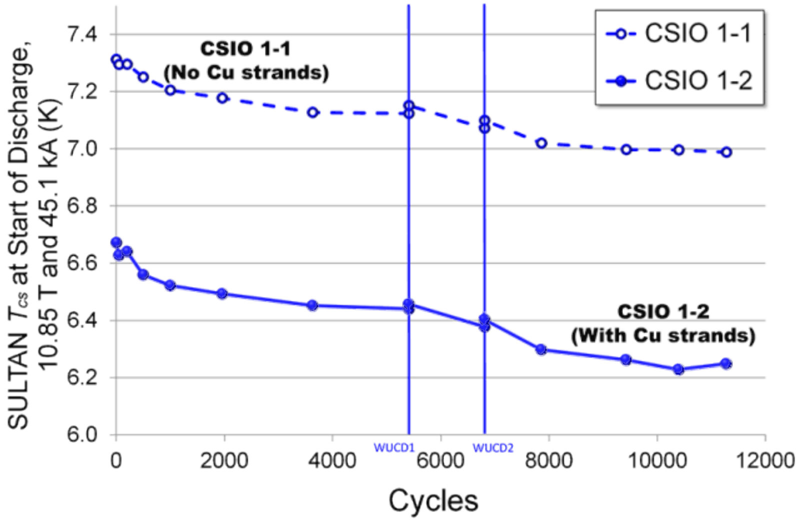

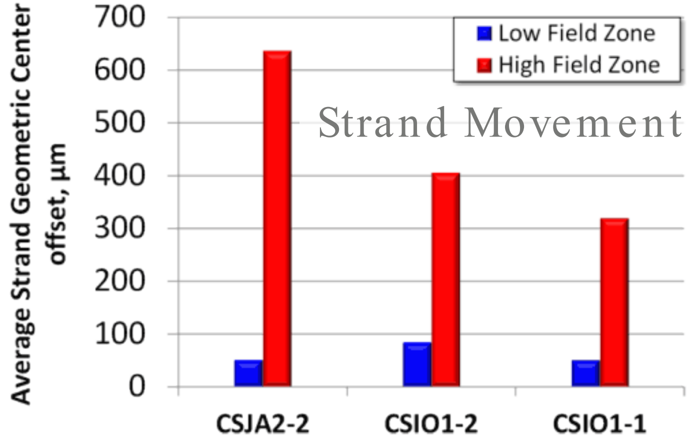

After cyclic testing in the SULTAN facility we analyze this cross section to show strand movement caused by the immense Lorentz force.

Strands are shaded according to the adjacent strand count, which ranges from zero to 5 (most densely packed ≤ 2.5 µm separation).

Sultan-tested cable courtesy of courtesy of Pierluigi Bruzzone (Plasma Physics Research Center) with agreement from US ITER.

iter
china eu india japan korea russia usa

Powder In Tube processed Nb_3Sn superconducting wires

- For FCC application, PIT strands offer the potential of both high-J_c and small effective filament diameter
- Composite wires are 156 or 192 superconducting filaments stacked into a Cu stabilizer matrix.
  - Ideally filaments are perfectly circular with the Sn-rich core centered in the Nb-Ta reaction tube
    - The superconducting A15 phase is formed when the Sn diffuses radially outward into the Nb-Ta tube which houses it.

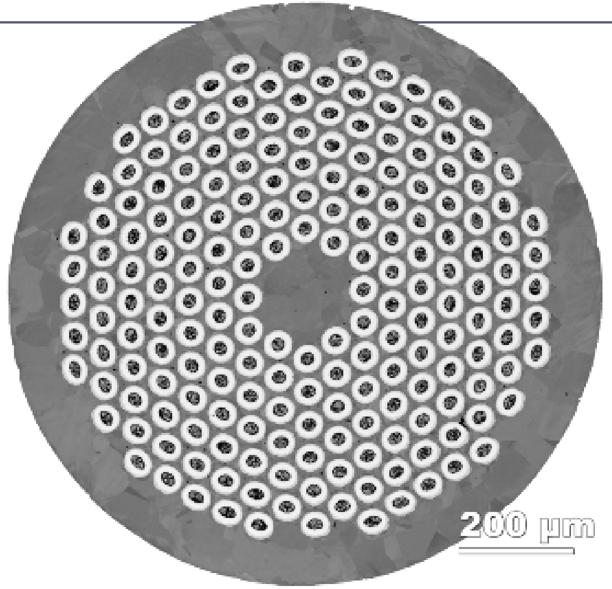

- Unfortunately, the filaments undergo non-uniform deformation during wire manufacture which leads to:
  - Ellipticity
  - Sn core drifting from center of Nb-Ta tube.
  - Reduced A15 volume
  - Reduced RRR

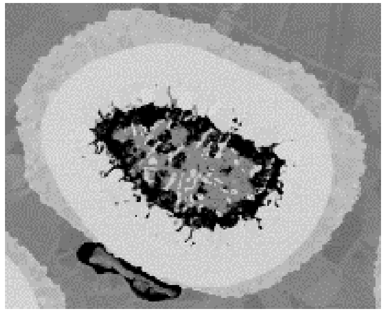

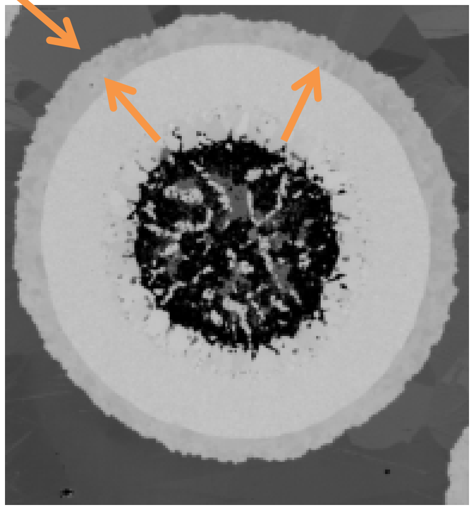

reacted

From Chris Segal

IEEE CSC & ESAS SUPERCONDUCTIVITY NEWS FORUM (global edition), February 2019.
Plenary presentation 3PL1A-01 given at ASC 2018, October 28-November 02, 2018, Seattle, (USA).

What's keeping PIT…in the pit

Shape analysis shows non-uniform deformation negatively impacting electrical stability as Sn leaks can

- Reduce RRR
- Reduce A15 volume
  - lower J_c

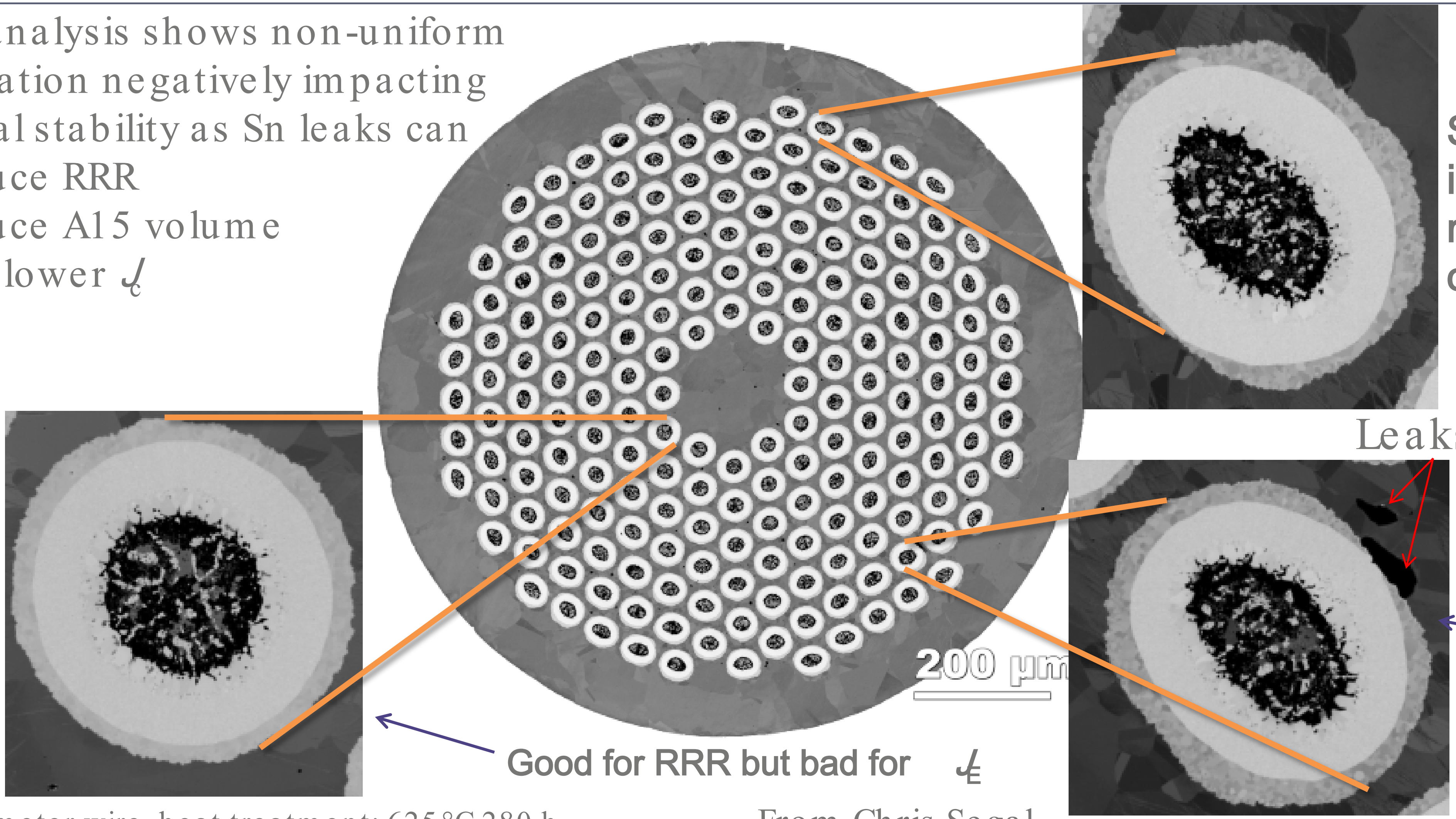

1 mm diameter wire, heat treatment: 625 °C 280 h

From Chris Segal

Filaments show a wide distribution of barrier thickness

-Bad for RRR, and bad for A15 formation

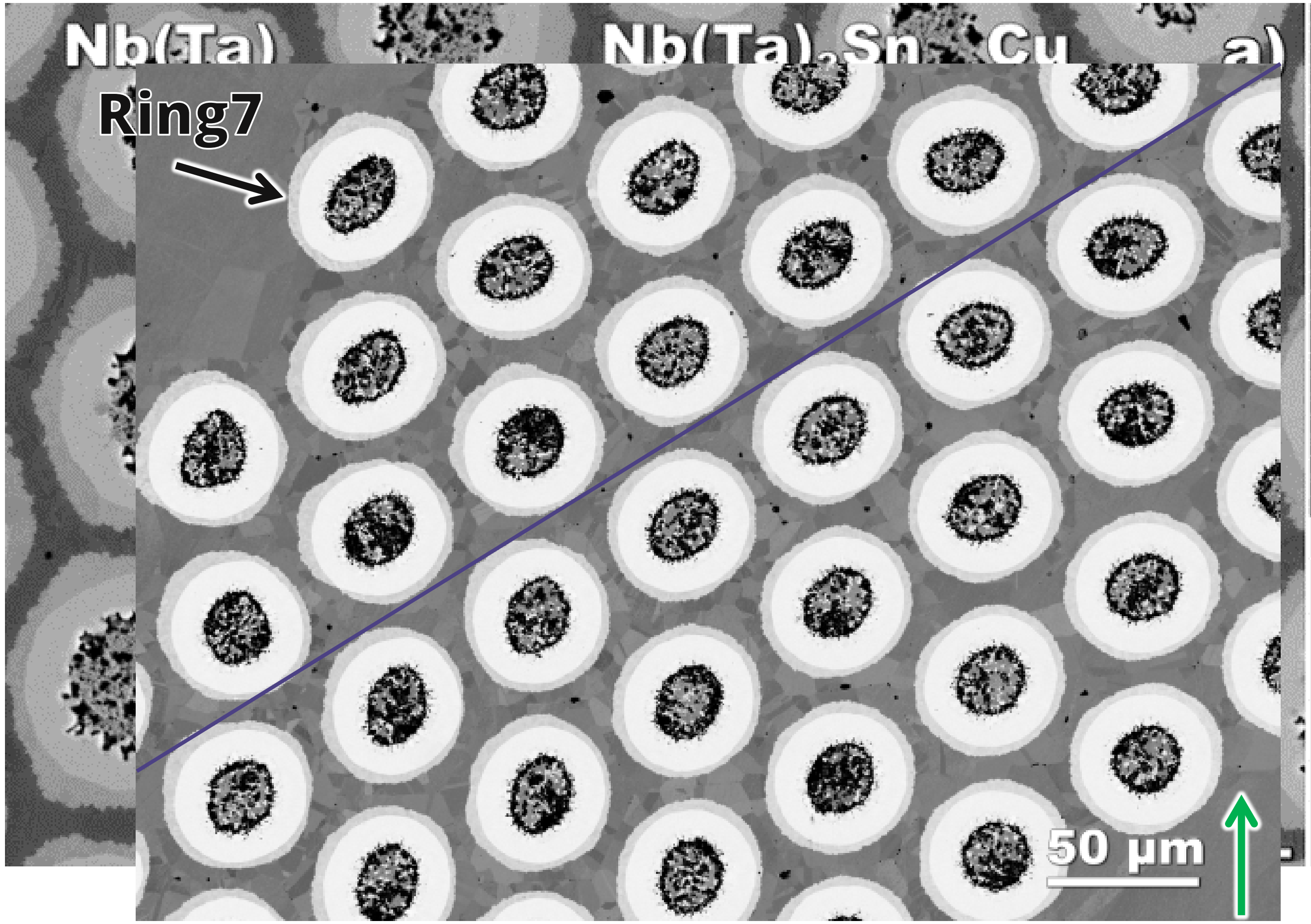

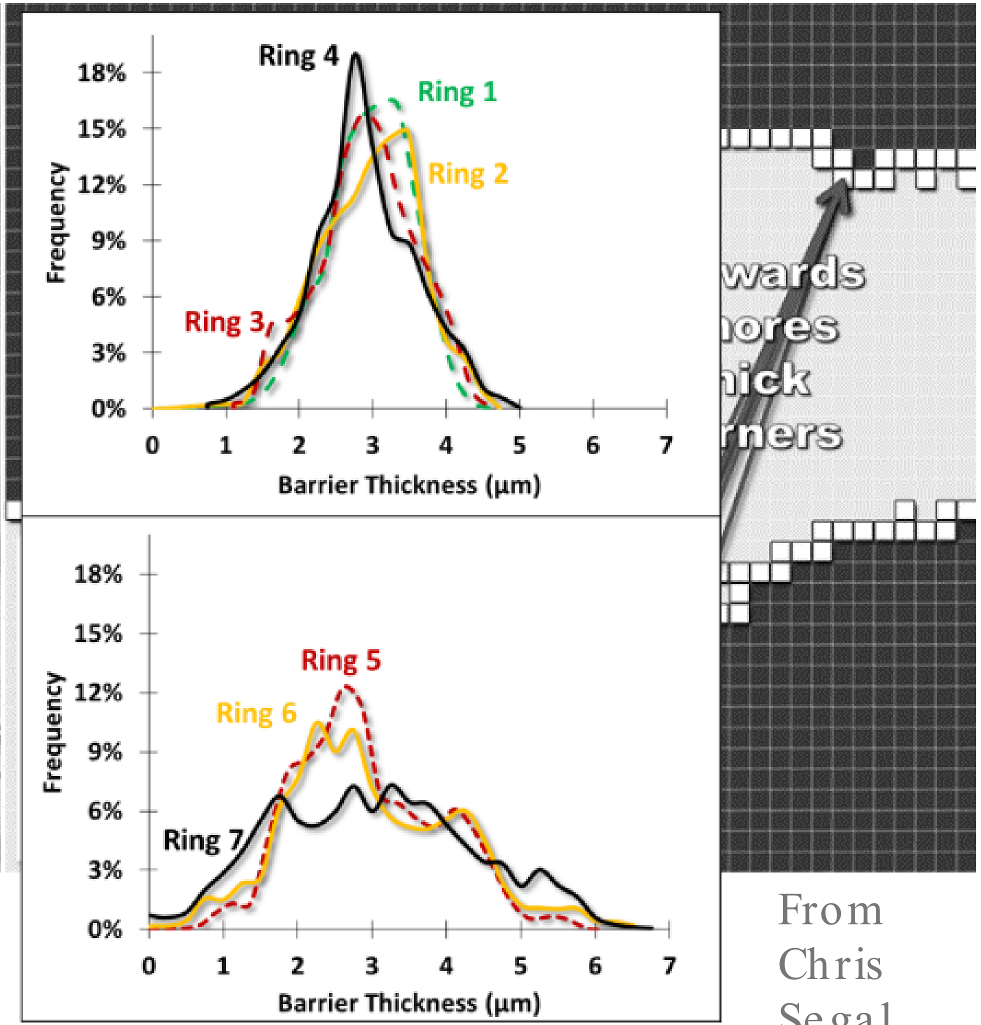

What is the mechanism that causes thinned regions of diffusion barrier?

From Chris Segal

Centroid drift between Nb-Ta tube and powder core can cause leaks

Two main issues

- Filaments become more elliptical as the wire is processed to final size, outer filaments much more than inner [1][2][3].
- The powder core deforms at a different rate than the Nb-Ta tube housing it, causing the centers to drift from one another.
  - This creates an uneven reaction front.

How do we measure it

- The centroid drift is the distance between the centroid of the entire filament (orange) and the centroid of the A15 layer (green)
- To most accurately compare between filaments and wires, we normalize each filament's core offset to its own effective diameter, derived from its area.

1.5 µm (4.2% of diameter)

Thick side

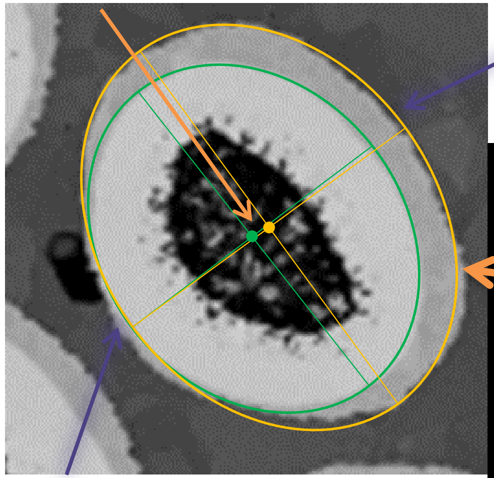

Thin side

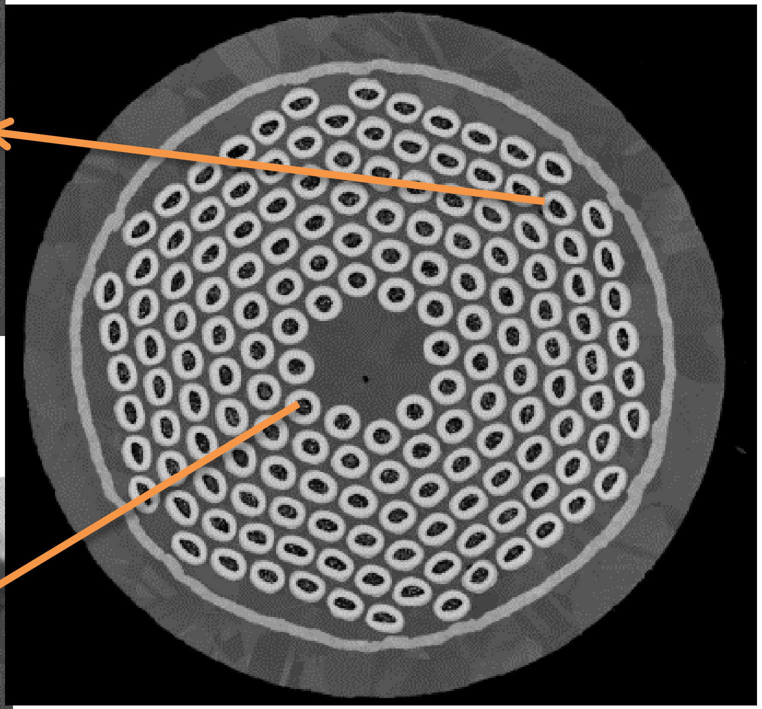

72 nm (0.2% diameter)

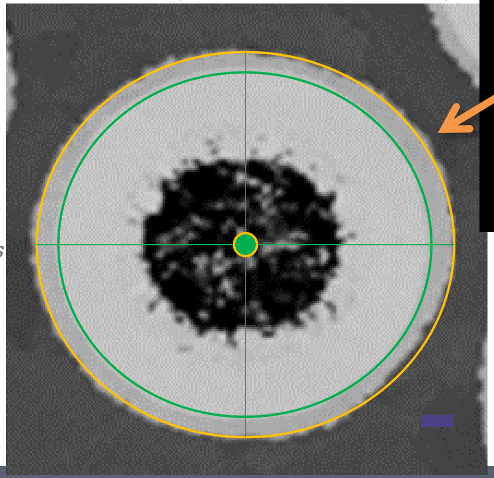

0.7 mm wire diameter, 36 µm filament diameter

From Chris Segal

[1] Segal, C.; Tarantini, C.; Lee, P. and Larbalestier, D., *Observations of Local Barrier Breakdown in PIT Wires and its Effect on RRR*, Low Temperature Superconductivity Workshop (LTSW), St. Petersburg, FL, November 4-6 (2013)
[2] Segal, C.; Tarantini, C.; Lee, P.J. and Larbalestier, D.C., *Novel Methods for Improving Nb_3Sn Powder in Tube Conductors for the FCC and Beyond*, Cryogenic Engineering Conference and International Cryogenic Materials Conference, (CEC-ICMC), Madison, WI July 9-12 (2017)
[3] C. Segal *et al.*, "Evaluation of critical current density and residual resistance ratio limits in powder in tube Nb_3Sn conductors," *Supercond. Sci. Technol.*, vol. 29, no. 8, p. 85003, 2016.

How does centroid drift in a filament change along length?

4 cm length tomography

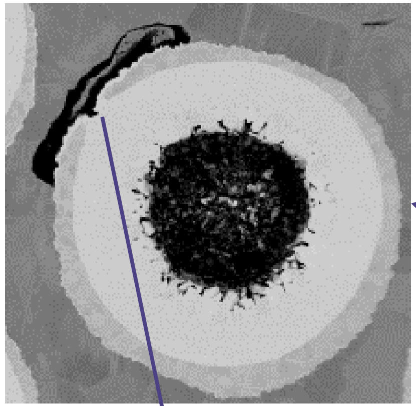

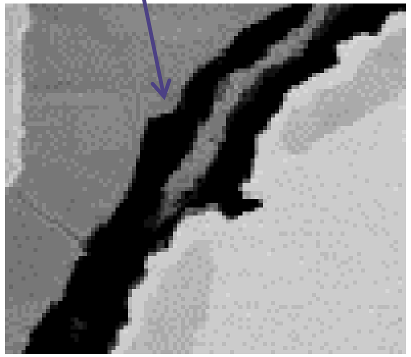

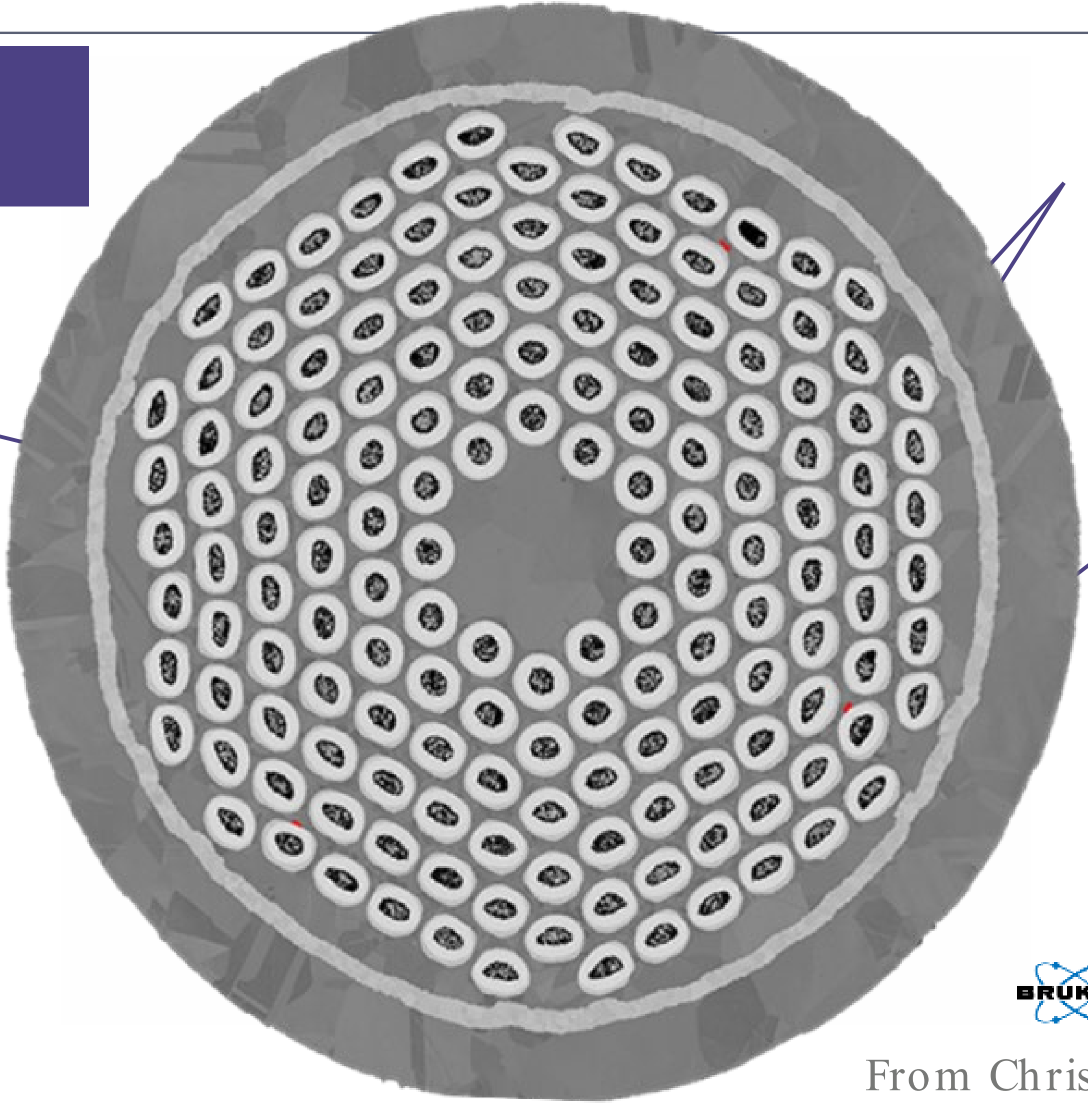

1. Filament has large color change between frames
   - Implies local defect or instability
2. Filament is similar color all the way through

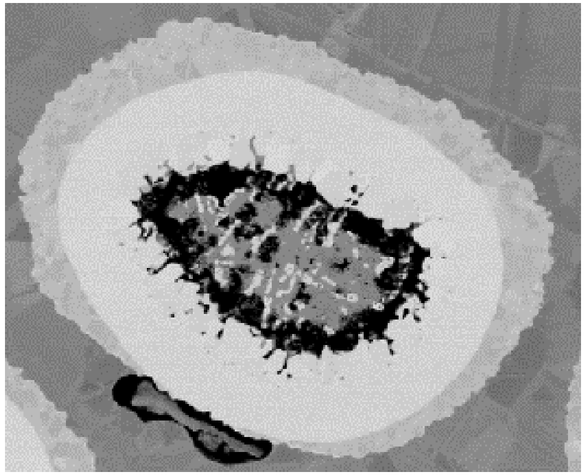

From Chris Segal

Serial section tomography: Leak distribution of each filament over 4 cm

Filaments with Kirkendall voids are plentiful along the entire 4 cm of wire, marked in black and integrated over 8 images

- Higher frequency in the external rings
- About half of the filaments leak enough Sn to produce a Kirkendall void in the 4 cm length.
  - In some cases the Kirkendall void may be centimeters long

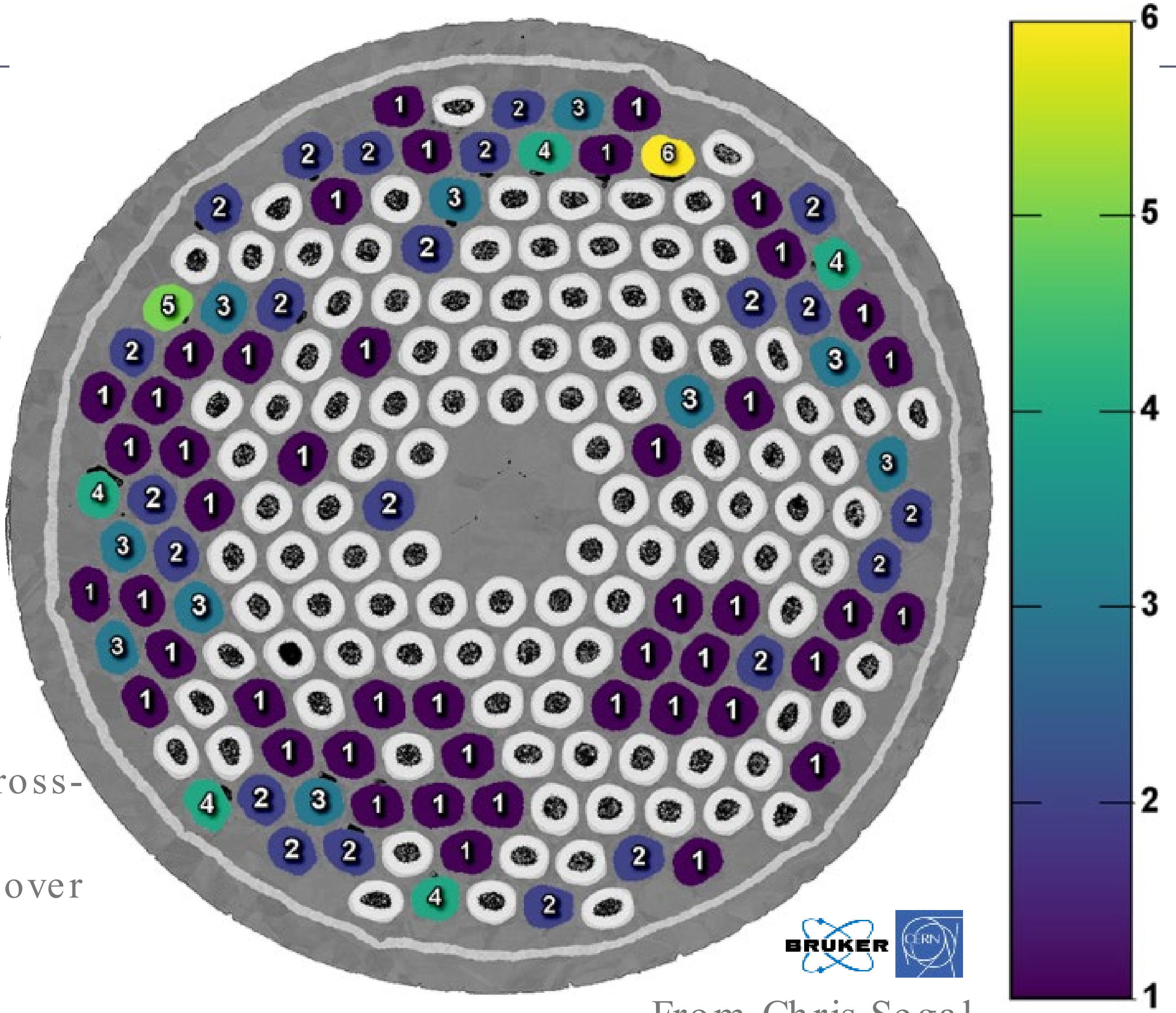

- Bernd 0.7 mm wire, very high Sn
- 15-20 Kirkendall void leaks in any given cross-section
- 81 leaked filaments with Kirkendall voids over 4 cm
- (8 cross sections over 4 cm)

From Chris Segal

X-ray microtomography: ESRF Grenoble

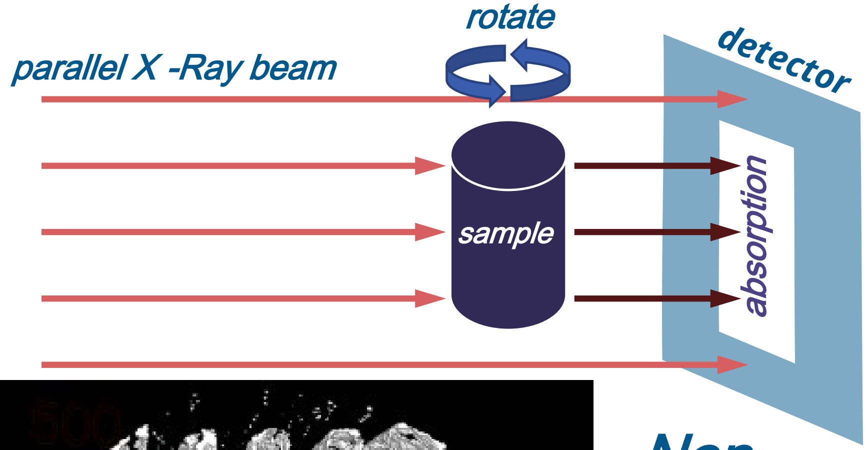

- X-ray photon energy = 89 keV
- 360° rotation of the sample
- 30000 projections
- 2560 x 2160 pixels
- 0.57 μm/pixel resolution

ESRF
The European Synchrotron

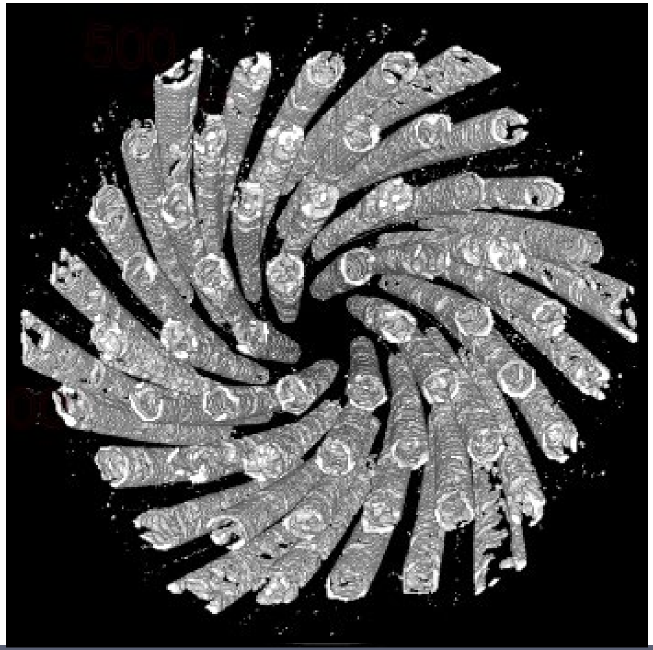

Non-destructive 3D volume reconstruction with separation of internal features

SCIENTIFIC REPORTS

OPEN

Quantitative correlation between the void morphology of niobium-tin wires and their irreversible critical current degradation upon mechanical loading

C. Barth[1], B. Seeber[2], A. Rack[3], C. Calzolaio[1], Y. Zhai[4], D. Matera[1] & C. Senatore[1]

[1]Department of Quantum Matter Physics (DQMP), University of Geneva, Geneva, Switzerland. [2]Department of Applied Physics (GAP), University of Geneva, Geneva, Switzerland. [3]European Synchrotron Radiation Facility (ESRF), Grenoble, France. [4]Princeton Plasma Physics Laboratory (PPPL), Princeton University, Princeton, NJ, USA. Correspondence and requests for materials should be addressed to C.B. (email: christian.barth@unige.ch)

SCIENTIFIC REPORTS | (2018) 8:6589 | DOI:10.1038/s41598-018-24966-z

Slide courtesy of Carmine Senatore (U-Geneva) not to be redistributed without request

UNIVERSITÉ DE GENÈVE
FACULTÉ DES SCIENCES
CERN

Reconstruction of the voids inside Nb_3Sn sub-elements by X-ray microtomography

ASC'18 2MOr01-02

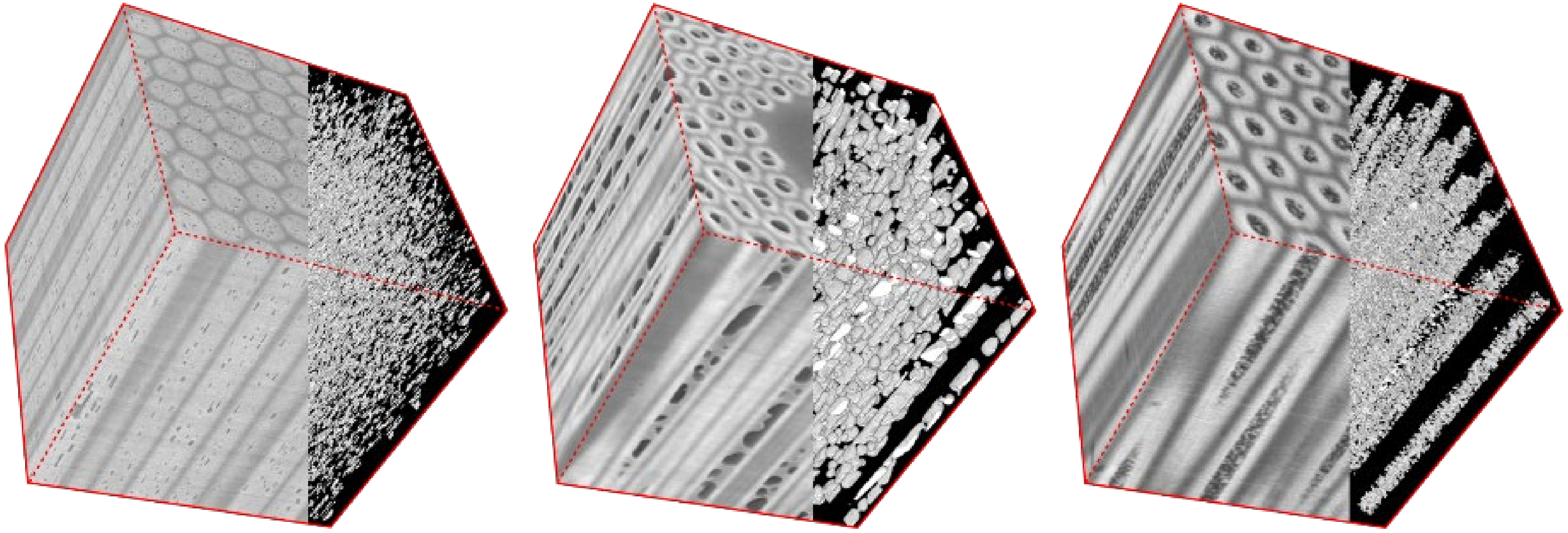

Statistical analysis of void size, shape and orientation

Slide courtesy of Carmine Senatore (U-Geneva) not to be redistributed without request

Bronze Route	***Internal Sn***	***PIT***
121 x 121 filaments	*132/169 sub-elements*	*192 filaments*

Scaling behavior of the critical current under transverse stress in RRP and PIT Nb_3Sn wires

Carmine SENATORE, Christian BARTH, Luc GAMPERLE
Department of Quantum Matter Physics, University of Geneva, Switzerland

UNIVERSITÉ DE GENÈVE
FACULTÉ DES SCIENCES

Jose FERRADAS, Bernardo BORDINI, Davide TOMMASINI
CERN, Switzerland

CERN

TEM has also advanced with field emission sources and aberration correction . . . No more dark rooms/wet developers!

1MOr2B-06: Shreyas Balachandran et al. : Ta-Hf doped Nb_3Sn for very high J_c

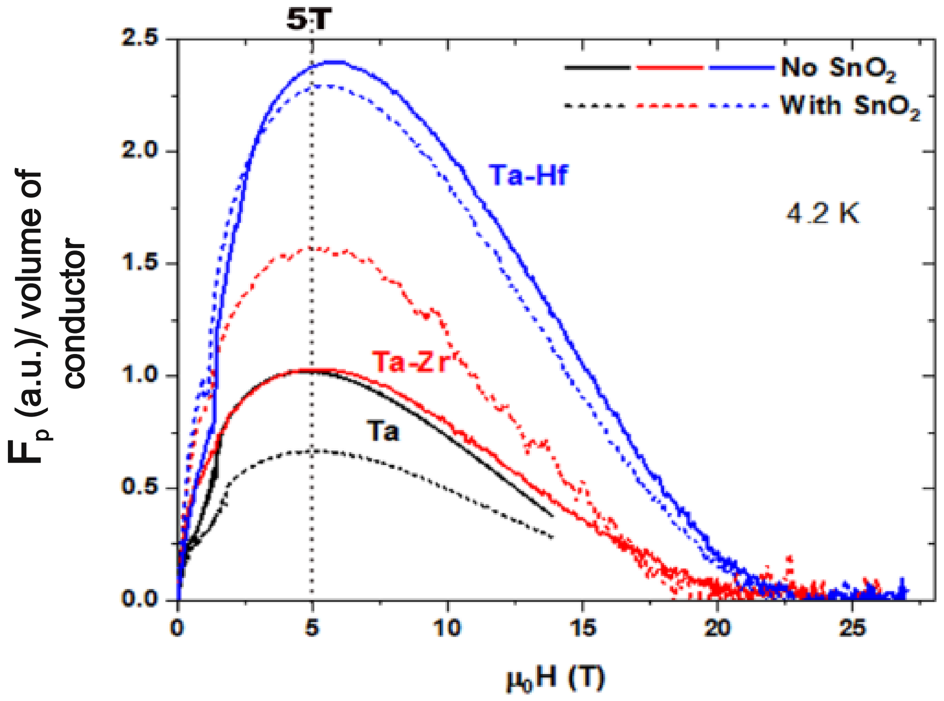

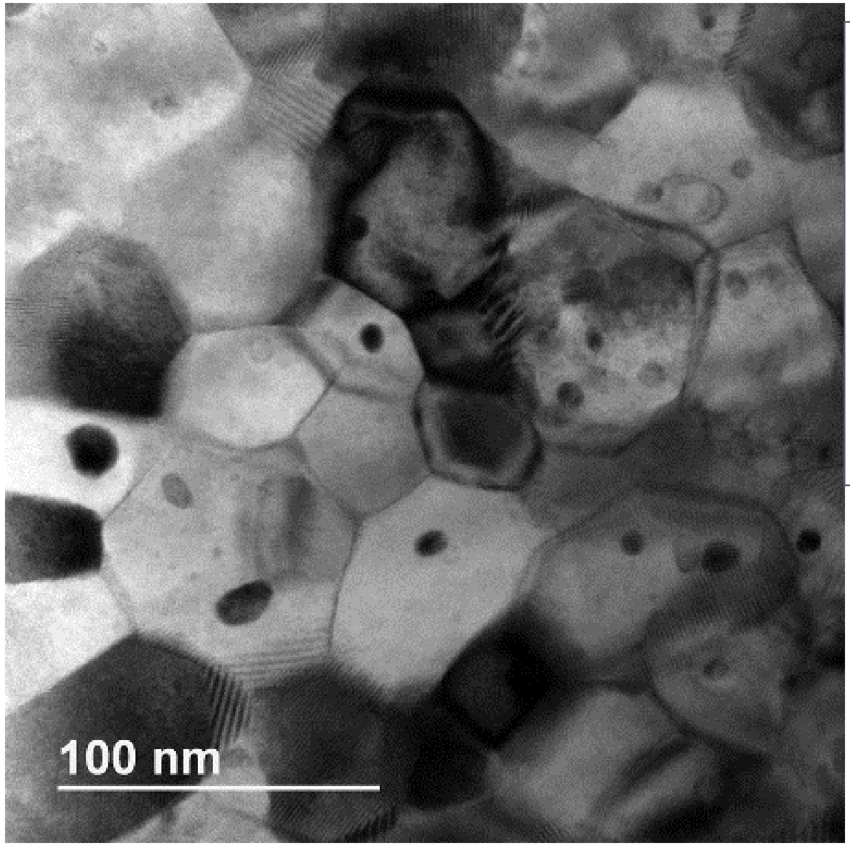

http://arxiv.org/abs/1811.08867 S. Balachandran *et al.*, "Beneficial influence of Hf and Zr additions to Nb4at.%Ta on the vortex pinning of Nb_3Sn with and without an O source," *arXiv:1811.08867 [cond-mat]*, Nov. 2018.

- Preliminary TEM-EELS microanalysis suggests that these precipitates are Ta rich, and Sn deficient.

U.S. MAGNET DEVELOPMENT PROGRAM · U.S. DEPARTMENT OF ENERGY | Office of Science · CERN

We have come a very long way

- But we still hope to see more surprises like Ta–Hf doped Nb_3Sn
- And perhaps even explain them using more advances in microscopy techniques.

- This work was supported by multiple awards from U.S. Department of Energy, ITER and CERN. A portion of this work was performed at the National High Magnetic Field Laboratory, which is supported by National Science Foundation Cooperative Agreement No. DMR-1157490 (-2017) DMR-1644779 (2018-) and the State of Florida.